

1 **Hysteresis in PIF4 and ELF3 dynamics dominates warm daytime memory in**  
2 **Arabidopsis**

3  
4 Germán Murcia<sup>1</sup>, Cristina Nieto<sup>2,4</sup>, Romina Sellaro<sup>3,4</sup>, Salomé Prat<sup>2</sup> and Jorge J. Casal<sup>1,3,\*</sup>

5  
6  
7 \*Author for correspondence: [casal@ifeva.edu.ar](mailto:casal@ifeva.edu.ar)

8  
9 <sup>1</sup>Fundación Instituto Leloir, Instituto de Investigaciones Bioquímicas de Buenos Aires-  
10 CONICET, Buenos Aires, Argentina;

11 <sup>2</sup>Plant Molecular Genetics Department, CNB-CSIC, Darwin 3, 28049 Madrid, Spain

12 <sup>3</sup>Universidad de Buenos Aires, Consejo Nacional de Investigaciones Científicas y Técnicas,  
13 Instituto de Investigaciones Fisiológicas y Ecológicas Vinculadas a la Agricultura (IFEVA),  
14 Facultad de Agronomía, Buenos Aires, Argentina;

15 <sup>4</sup>These authors contributed equally to this work

16  
17  
18  
19 Short title: Growth memory of warm daytime

20  
21 The authors responsible for distribution of materials integral to the findings presented in this  
22 article in accordance with the policy described in the Instructions for Authors  
23 (<https://academic.oup.com/plcell/pages/General-Instructions>) are: Jorge J. Casal  
24 ([casal@ifeva.edu.ar](mailto:casal@ifeva.edu.ar)) and Salomé Prat ([salome.prat@cragenomica.es](mailto:salome.prat@cragenomica.es)).

25

26 **Abstract**

27 Plants may experience large diurnal temperature fluctuations. Our knowledge of the  
28 molecular mechanisms of integration of these fluctuations and the resulting growth patterns is  
29 limited. Here we show that hypocotyl growth during the night responded not only to the  
30 current temperature but also to preceding daytime temperatures, revealing a memory of  
31 previous conditions. Daytime temperature affected the nuclear levels of PHYTOCHROME  
32 INTERACTING FACTOR 4 (PIF4) and LONG HYPOCOTYL 5 (HY5) during the next night.  
33 These jointly accounted for the observed growth kinetics, whereas memory of prior daytime  
34 temperature was impaired in the *pif4* and *hy5* mutants. *PIF4* promoter activity largely  
35 accounted for the temperature dependent changes in PIF4 protein levels. Noteworthy, the  
36 decrease in *PIF4* promoter activity triggered by cooling required a stronger temperature shift  
37 than the increase caused by warming. This hysteretic pattern required EARLY-FLOWERING  
38 3 (ELF3). Warm temperatures promoted the formation of nuclear condensates of ELF3 in  
39 hypocotyl cells during the afternoon but not in the morning. These nuclear speckles showed  
40 poor sensitivity to subsequent cooling. We conclude that ELF3 achieves hysteresis and drives  
41 the *PIF4* promoter into the same behaviour, enabling a memory of daytime temperature  
42 conditions.

43  
44  
45

## 46 **Introduction**

47

48 Warmer temperatures within the physiological range can selectively increase or decrease the  
49 growth of different organs, leading to modifications in plant architecture or  
50 thermomorphogenesis (Quint et al., 2016; Casal and Balasubramanian, 2019).

51 Thermomorphogenesis occurs in crop species, highlighting the need to understand this  
52 process in further deepness in the current context of global warming (Casal and  
53 Balasubramanian, 2019). A well-established model in thermomorphogenesis, useful to  
54 understand the basic mechanisms, is the enhanced growth of the hypocotyl in *Arabidopsis*  
55 *thaliana* seedlings in response to non-stressful warm temperatures (Gray et al., 1998).

56 The photo-sensory receptor phytochrome B (phyB) (Jung et al., 2016; Legris et al.,  
57 2016), the clock protein EARLY FLOWERING 3 (ELF3) (Jung et al., 2020) and the  
58 transcription factor PHYTOCHROME INTERACTING FACTOR 7 (PIF7) (Chung et al., 2020)  
59 are the three plant temperature sensors involved in the control of hypocotyl growth identified  
60 so far. Warm temperatures accelerate the rate of thermal reversion of active phyB to its  
61 inactive conformer (Jung et al., 2016; Legris et al., 2016; Burgie et al., 2021). ELF3 is a  
62 component of the evening complex and warm temperatures reduce its binding to the target  
63 gene promoters (Box et al., 2015; Ezer et al., 2017; Silva et al., 2020). ELF3 contains a  
64 predicted prion domain with a polyglutamine repeat, which is important for the reversible  
65 phase transition from active to the inactive state of ELF3 under warm conditions (Jung et al.,  
66 2020). According to Jung et al. (2020), warm temperatures can enhance the formation of  
67 nuclear speckles containing ELF3, but Ronald et al. (2021) reported the opposite pattern.  
68 Therefore, there is controversy about the link between these a sub-nuclear bodies and ELF3  
69 activity. Warmth-induced changes in the RNA hairpin present at the 5'-untranslated region of  
70 the *PIF7* transcript favour its translation, increasing PIF7 protein abundance (Chung et al.,  
71 2020). phyB and ELF3 signalling converge on PIF4, as phyB physically interacts and  
72 negatively regulates PIF4 protein stability (Cheng et al., 2021) and the evening complex binds  
73 the *PIF4* gene promoter reducing its expression during early night (Nusinow et al., 2011).  
74 Therefore, both *PIF4* expression (Koini et al., 2009; Stavang et al., 2009; Box et al., 2015)  
75 and PIF4 protein stability (Foreman et al., 2011) increase under elevated temperatures. In  
76 addition, ELF3 sequesters PIF4 by direct physical interaction preventing PIF4 binding to its  
77 transcriptional targets (Nieto et al., 2015).

78            CONSTITUTIVELY PHOTOMORPHOGENIC 1 (COP1), ELONGATED HYPOCOTYL  
79 5 (HY5) and LONG HYPOCOTYL IN FAR-RED (HFR1) are among the several regulators of  
80 PIF4 activity. COP1 is a RING E3 ligase that is required for the hypocotyl growth response to  
81 warm temperatures (Delker et al., 2014). Warm temperature increases nuclear accumulation  
82 of COP1 (Park et al., 2017) and this enhances the expression of *PIF4* (Gangappa and Kumar,  
83 2017). HY5 binds the *PIF4* promoter to negatively regulate its activity (Delker et al., 2014).  
84 HY5 also competes with PIF4 in its binding to the target gene promoters (Toledo-Ortiz et al.,  
85 2014), while warm temperatures inhibit the expression of the *HY5* gene and can lower the  
86 HY5 protein stability (Catalá et al., 2011; Delker et al., 2014; Toledo-Ortiz et al., 2014). HFR1  
87 is stabilised under warm temperatures (Romero-Montepaone et al., 2021) and inhibits PIF4  
88 and PIF7 binding to its targets, by direct physical interaction (Hornitschek et al., 2009; Sandi  
89 Paulišić et al., 2021). The transcription factor PIF4 (Crawford et al., 2012; Sun et al., 2012)  
90 and PIF7 (Fiorucci et al., 2020) transcription factors bind auxin synthesis gene promoters to  
91 increase auxin levels in the warmth. Auxin produced in the cotyledons travels down to the  
92 hypocotyl to promote growth (Bellstaedt et al., 2019).

93            In nature, temperatures typically fluctuate between day and night. We have recently  
94 observed that night temperature information stored in phyB affects hypocotyl growth during  
95 the subsequent photoperiod (Murcia et al., 2020). However, we ignore whether the reciprocal  
96 control is also true; i.e. whether temperature responsive hypocotyl elongation at night  
97 depends on the temperature experienced during the preceding photoperiod. Here we report  
98 that nighttime hypocotyl growth and gene expression depend not only on the temperature  
99 during the night itself but also on former daytime temperature.

100

## 101 **Results**

102

### 103 **Nighttime growth depends on daytime temperatures**

104

105 To investigate whether the growth of the hypocotyl during the night responds exclusively to  
106 the current temperature or is also affected by the conditions experienced during the previous  
107 photoperiod, plants of the Col wild type (WT) were exposed to all possible combinations  
108 between three daytime temperatures and three nighttime temperatures (10, 20 and 28°C).  
109 Furthermore, to analyse whether the status of photo-sensory receptors modify the influence of  
110 previous temperature, plants were exposed to simulated sunlight or shade conditions during

111 daytime and either a far-red light pulse (EOD FR, 10 min) or no light pulse at dusk. As  
112 expected, warmer nights accelerated nighttime growth (Fig. 1A, Table S1A). More  
113 importantly, for all nighttime conditions, warmer daytime temperatures caused faster nighttime  
114 growth (Fig. 1 A, Table S1A). EOD FR or daytime shade accelerated hypocotyl growth during  
115 the night (Table S1A). Significant interactions indicate that the effect of daytime temperature  
116 was stronger when nighttime temperatures were warmer and in seedlings exposed to EOD  
117 FR (Table S1A). Taken together, these results indicate that nighttime growth depends not  
118 only on the nighttime temperature itself but also on prior daytime temperature, particularly  
119 under the conditions that elicit faster nighttime growth (warm night, daytime shade, EOD FR).  
120 Based on these observations, in subsequent experiments we used daytime shade and EOD  
121 FR to optimise the analysis. This phenomenon should not be confused with the known effects  
122 of day / night temperature differentials, which actually impact on daytime growth (Bours et al.,  
123 2013, 2015).

124 To obtain a detailed kinetics of nighttime growth, we exposed the seedlings to two  
125 different temperatures during the day (10 and 28°C) and two different night temperatures (10  
126 and 28°C) in all four combinations. Hypocotyl growth rate responded to current and previous  
127 temperature conditions (Fig. 1B, Table S1B). After the initial 4 h of the night, hypocotyl growth  
128 proceeded at a constant rate, indicating that the transition interval had ended by then.  
129 However, growth rate remained significantly affected by previous temperatures beyond that  
130 point (Fig. 1B). In effect, according to a multiple regression analysis, hypocotyl length  
131 increase between ZT= 14 h and ZT= 22 h depended on time (coefficient  $\pm$ SE,  $4.4 \text{ E-}03 \pm 1.4\text{E-}$   
132  $03$ ,  $p=0.0025$ ), the interaction between time and night temperature ( $0.04 \pm 1.4\text{E-}03$ ,  $p$   
133  $<0.0001$ ), and the interaction with daytime temperature ( $0.01 \pm 1.4\text{E-}03$ ,  $p <0.0001$ ). These  
134 observations indicate that the daytime cue remains stored in the system, persistently affecting  
135 growth. In plants that experienced a cold day, a warm night did not increase hypocotyl growth  
136 to the rates exhibited by plants already exposed to warmth during the day. Conversely, in  
137 plants that experienced a warm day, a cold night did not decrease hypocotyl growth to the  
138 rates exhibited by plants already exposed to cold temperature during the day.

### 139 140 **Nighttime gene expression depends on daytime temperatures**

141  
142 Prompted by these interaction effects we investigated whether nighttime gene expression  
143 depended on daytime temperatures. We used transgenic lines bearing the *pPIL:LUC* or

144 *pIAA19:LUC* promoter-reporter fusions in seedlings grown at two different temperatures  
145 during the day (10 and 28°C) and two different night temperatures (10 and 28°C) in all four  
146 combinations. For both promoters, the activities in seedlings transferred from 10 to 28°C did  
147 not reach the levels observed in seedlings exposed to 28°C day and night; and in the  
148 seedlings transferred from 28 to 10°C did not drop to the levels observed for those exposed to  
149 10°C day and night (Fig. 2A-B, Table S1C-D). Noteworthy, a cold night did not cause any  
150 reduction in the activity of the *pPIL:LUC* promoter after a warm day. Therefore, not only  
151 growth but also gene expression showed effects of daytime temperature that persisted during  
152 the night.

153

### 154 **Genetic requirement of daytime temperature effects on nighttime growth**

155

156 We compared the WT to different mutants to gain insight into the genetic requirements for the  
157 effect of daytime temperature on nighttime growth. We grew seedlings at 28°C or 10°C and  
158 exposed them to shade during daytime, followed by EOD FR. In a first set of experiments, we  
159 exposed all the seedlings to 28°C during the night. The WT showed faster growth during the  
160 night when subjected to the warmer temperature during daytime (Fig 3A-B, Table S1E). The  
161 *pif4*, *pif7* and *hfr1* mutants showed a reduced response to daytime temperature and the *cop1*,  
162 *elf3* and *hy5* mutants showed an inverted response. The *pif5* mutation did not reduce the  
163 effect of daytime temperature and actually partially rescued the defect of *pif4* and *pif7* (Fig.  
164 S1, Table S1E). In a second set of experiments, we exposed all the seedlings to 10°C during  
165 the night. Loss of effects of daytime temperature were observed in the *cop1*, *pif4*, *pif5*, *pif7*  
166 and *hy5* mutants (Fig 3C-D, Table S1F).

167

### 168 **Memory of daytime temperature in the status of signalling components**

169

170 The *pif4*, *pif7*, *hfr1*, *cop1*, *elf3* and *hy5* mutants did not show the normal enhancement of  
171 nighttime growth by warm daytime temperatures observed in the WT. Therefore, we  
172 investigated the status of these signalling components by 4 h into the night (ZT= 14 h, 28°C)  
173 in seedlings exposed to contrasting daytime temperatures (10 and 28°C).

174 Warm temperatures increase the nuclear levels of PIF4 (Legris et al., 2017) and COP1  
175 (Park et al., 2017) and decrease the nuclear levels of HY5 (Romero-Montepaone et al.,  
176 2021). We used confocal microscopy to analyse the nuclear fluorescence of *pPIF4:PIF4-GFP*,

177 *pHY5:HY5-YFP* and *p35S:YFP-COP1* transgenic lines. At 28°C, nuclear abundance of PIF4  
178 and COP1 in the night was increased and that of HY5 was reduced in the hypocotyl cells of  
179 seedlings that had received 28°C compared to 10°C during the day (Fig. 4A-F).

180 Warm temperatures were described to increase (Jung et al., 2020) or decrease  
181 (Ronald et al., 2021) the formation of nuclear speckles containing ELF3. Since  
182 overexpression of ELF3 has no effect on temperature responsiveness compared to the WT  
183 (Thines and Harmon, 2010; Jung et al., 2020), we used the *p35S:YFP-ELF3* line to facilitate  
184 the quantitative analysis of the ELF3 speckles (the same line used by Ronald et al., 2021).  
185 We observed a significantly higher number of ELF3 speckles in the seedlings exposed to  
186 28°C than in seedlings exposed to 10°C during the day (Fig. 4G-H).

187 Warm temperatures increase PIF7 protein levels (Fiorucci et al., 2020; Chung et al.,  
188 2020) and enhance HFR1 protein stability (Romero-Montepaone et al., 2021). However,  
189 protein blot analyses of seedlings sampled after four hours into the 28 °C night did not reveal  
190 differences in PIF7 protein abundance caused by contrasting daytime temperatures (Fig. 4I-  
191 J). Similarly, in luminometer readings, we did not observe significant effects of daytime  
192 temperature on nighttime *HFR1* promoter activity or HFR1 stability (Fig. 4K-L).

193 PIF4 and COP1 promote hypocotyl growth whereas HY5 inhibits hypocotyl growth  
194 during the night (e.g. Fig. 3). Cold days decreased PIF4 and COP1 nighttime activities and  
195 increased HY5 nighttime activities (Fig. 4A-F), suggesting that PIF4, HY5, and COP1 convey  
196 daytime temperature information to nighttime growth. This would also be the case for ELF3 if  
197 enhanced speckle formation correlates with reduced activity, a link analysed in further detail  
198 below. Conversely, the short-term memory of daytime temperature requires PIF7 and HFR1  
199 (Hornitschek et al., 2009; Sandi Paulišić et al., 2021), but apparently, these factors do not  
200 carry prior temperature information because their levels during the night showed no influence  
201 of daytime conditions (Fig.4I-L).

## 202 203 **Nighttime PIF4 and HY5 kinetics account for growth responses**

204  
205 Since ELF3 and COP1 control hypocotyl growth partially via PIF4 and HY5 (Gangappa and  
206 Kumar, 2017; Park et al., 2017; Nusinow et al., 2011; Box et al., 2015), we analysed in further  
207 detail the nighttime kinetics of nuclear abundance of these two transcription factors by using  
208 confocal microscopy of hypocotyl cells. The seedlings exposed to 28°C during the day,  
209 compared to 10°C, during the day, initiated the night with more PIF4 and less HY5 in the

210 nucleus of their hypocotyl cells and these differences persisted at least during several hours  
211 (Fig. 5A-D). The seedlings that were transferred at the beginning of the night from 10°C to  
212 28°C reached similar PIF4 or HY5 nuclear levels as those kept at 28°C during daytime by 8 h  
213 after the temperature shift (ZT= 18 h, Fig. 5A-D). In seedlings transferred from 28°C to 10°C,  
214 similar HY5 nuclear levels as in the seedlings already exposed to 10°C during daytime were  
215 only observed 12 h later (ZT= 22 h, Fig. 5C-D). Noteworthy, 28°C to 10°C shift at the  
216 beginning of the night caused almost no PIF4 response (Fig. 5A-B). Taken together, these  
217 results indicate that the nighttime kinetics of PIF4 and HY5 depend on both nighttime and  
218 daytime temperature (Table S1G-H). Differences in their protein levels caused by the  
219 contrasting temperatures during the day extended several hours into the night, either due to a  
220 slower transitions between the levels typical of day and night temperatures (PIF4 from 10°C  
221 to 28°C and HY5 in both directions) or a nearly complete insensitive response (PIF4 from  
222 28°C to 10°C).

223 Genetic studies indicated that effects of daytime temperature effects depend on PIF4  
224 and HY5 (Fig. 3). Therefore, we explored the quantitative association between the growth rate  
225 kinetics of growth rate and that of PIF4 and HY5 nuclear levels by using multiple regression  
226 analysis across three temporal phases (ZT 10-14 h, 14-18 h and 18-22 h). For each temporal  
227 phase, we averaged the PIF4- or HY5- fluorescence values obtained by confocal microscopy  
228 at the beginning and the end of the phase (Fig. 5A and C) as explanatory variables. The  
229 model accounted for a significant proportion of the variability in growth rate (adjusted  $R^2=0.80$ ,  
230  $P < 0.0001$ ). Both PIF4 and HY5 levels contributed significantly (coefficient  $\pm$ SE, PIF4:  $2.1E-$   
231  $03 \pm 1.5E-04$ ,  $p < 0.0001$ ; HY5:  $-1.0E-03 \pm 3.2E-04$ ,  $p = 0.016$ ), indicating that the information  
232 that provided by PIF4 and HY5 dynamics is important and not redundant.

233 We also investigated the abundance of the PIF4 protein during the night by using  
234 transgenic lines bearing *pPIF4:PIF4-LUC*. As in the case of confocal microscopy analysis,  
235 there was little difference in PIF4 protein levels if the plants continued at 28°C or were shifted  
236 from 28°C to 10°C at the beginning of the night (Fig. 5E, Table S1I). Also resembling the  
237 hypocotyl pattern, PIF4 remained low throughout the night in plants grown at 10°C during the  
238 day and the night, and increased when plants were transferred from 10 °C to 28°C at the  
239 beginning of the night (Fig. 5E), although this response was faster than in the confocal  
240 studies. The upwards cotyledon signal dominates luminescence readings of entire seedlings;  
241 therefore, we used the line bearing the *pPIF4:PIF4-GFP* transgene to evaluate nuclear levels  
242 of PIF4 in cotyledon cells. The results confirmed elevated levels of PIF4 during the day (see



243 also Stavang *et al.*, 2009) and showed that these differences had already been inverted by 4  
244 h into the night (Fig. S2). The bioluminescence analysis of PIF4 levels in isolated hypocotyls  
245 of the *pPIF4:PIF4-LUC* line actually confirmed that the shift to 28°C at the beginning of the  
246 night was not enough to achieve the levels detected in this organ in seedlings grown at 28°C  
247 during the day (Fig. 5F).

248 Given the faster change in PIF4 levels in the cotyledons, we investigated whether the  
249 growth of this organ responds to daytime temperature in a PIF4-dependent manner. The area  
250 of the cotyledons increased more during the night at 28°C if the seedlings were exposed  
251 during daytime to 10°C (mean  $\pm$ SE,  $n=40$ ,  $4.0 \text{ E-}03 \pm 4.0 \text{ E-}04 \text{ mm}^2$ ), than when daytime  
252 temperature was 28°C ( $2.7 \text{ E-}03 \pm 2.1 \text{ E-}04 \text{ mm}^2$ ,  $P=0.005$ ). This memory effect was absent  
253 in the *pif4* mutant. Compared to the WT, *pif4* showed an enhanced cotyledon expansion with  
254 28°C daytime temperature ( $4.3 \text{ E-}03 \pm 4.8 \text{ E-}04 \text{ mm}^2$ ,  $P=0.0017$ ), similar to that observed at  
255 10°C ( $4.2 \text{ E-}03 \pm 4.8 \text{ E-}04 \text{ mm}^2$ ) (Huq and Quail, 2002). Therefore, differences in PIF4 levels  
256 in the cotyledons generated by 28°C compared to 10°C during the day, in spite of showing a  
257 shorter persistence during warm nights, convey daytime temperature information to nighttime  
258 growth of this organ.

259

### 260 ***PIF4* promoter activity accounts for PIF4 dynamics during the night**

261

262 Nighttime kinetics of *PIF4* promoter activity conserved the key features observed for the PIF4  
263 protein kinetics. It depended on nighttime and daytime activity and showed asymmetric  
264 responses to temperature shifts (Fig. 6A, Table S1L). The stronger *PIF4* promoter activity  
265 established by 28°C compared to 10°C during the day was largely irreversible during the  
266 night, as transfer to 10°C did not reduce this activity below the levels of 28°C controls (Fig.  
267 6A). Conversely, the seedlings transferred from 10°C to 28°C at the beginning of the night did  
268 increase the activity of the *PIF4* promoter (Fig. 6A). Luminescence readings driven by  
269 promoter and protein fusions showed strong correlation (Fig. 6B), supporting a major role of  
270 *PIF4* promoter activity in the control of nighttime PIF4 levels.

271 The nighttime patterns of PIF4 protein and *PIF4* promoter activities showed two  
272 features. The first feature is that daytime differences persisted at least several hours into the  
273 night. The second feature is the asymmetric response to temperature shifts in contrasting  
274 directions (increase compared to decrease in temperature). This asymmetric response to a

275 variable when it either increases or decreases its values is typical of hysteretic systems  
276 (Davies, 2017; Jiang and Hao, 2021).

### 277 278 **Daytime generation of night differences in PIF4 requires ELF3**

279  
280 The differences in PIF4 nuclear levels (Fig. 5A, C) and *PIF4* promoter activity (Fig. 6A) that  
281 persisted during the night were already present in the cotyledons and hypocotyls at the end of  
282 the day. We therefore investigated the processes involved in their generation during the  
283 photoperiod. Luminescence readings revealed that the abundance of PIF4 protein (Fig. 7A)  
284 and the activity of the *PIF4* promoter (Fig. 7B) abruptly increased early in the morning, when  
285 the seedlings were first transferred from 20°C to 28°C, compared to 10°C. Initial changes  
286 induced by such contrasting temperatures slightly narrowed down during the course of the  
287 day but were still present at the beginning of the night. The early increase in PIF4 protein  
288 signal at warm temperatures was more intense than that in *PIF4* promoter activity (cf. Fig 7A  
289 and B at 4 h), which is reflected by a higher protein / promoter activity ratio (Fig. 7C). The  
290 protein blot results using a line bearing the *p35S:PIF4-HA* transgene are consistent with a  
291 higher stability of PIF4 at 28°C than at 10°C early in the morning (Fig. S3A-B). However, later  
292 on in the day, PIF4 protein levels increased in the plants exposed to 10°C without a  
293 concomitant increment in *PIF4* promoter activity, causing a higher protein / promoter activity  
294 ratio in plants exposed to cooler temperatures (Fig. 7C). Therefore, the differences in PIF4  
295 protein levels at the beginning of the night were largely due to temperature effects on *PIF4*  
296 promoter activity, with only transient post-transcriptional effects.

297 We investigated whether differences in PIF4 observed at the end of the day require  
298 ELF3. Experiments using the lines bearing the *pPIF4:LUC* transgene in the *elf3* background  
299 indicated that, early in the photoperiod, warm temperature promoted *PIF4* activity even in the  
300 absence of ELF3 (Fig 7B), implying the action of other transcriptional regulators. However,  
301 temperature-induced changes in *PIF4* promoter activity showed an absolute requirement of  
302 ELF3 during the rest of the photoperiod (Fig 7B). During warm afternoons *PIF4* promoter  
303 activity declined, even in the *elf3* background (Figs 7B), and this might reflect an effect of  
304 GIGANTEA (Anwer et al., 2020).

305 Since luminometer readings of entire seedlings reflect *PIF4* promoter activity mainly in  
306 the cotyledons, we conducted experiments with isolated hypocotyls; i.e., the organ where  
307 differences in PIF4 are more persistent during warm nights (cf Figs 5C and E). The memory

308 of daytime temperatures of the *PIF4* promoter was also absent in the hypocotyl in the *elf3*  
309 background (Fig. 7D).

310

### 311 **Kinetics of ELF3**

312

313 We investigated the dynamics of ELF3 under the conditions where it controlled *PIF4* promoter  
314 activity. Under warm temperature, the formation of speckles decreased during the morning  
315 and increased strongly during the afternoon (Fig. 8A and C). In addition to *PIF4*, ELF3  
316 negatively regulates *TOC1* and positively regulates the *LHY* and *CCA1* promoters (Thines  
317 and Harmon, 2010; Fehér et al., 2011; Herrero et al., 2012; Ezer et al., 2017), in all cases  
318 through direct binding of these promoters. The activity of the *TOC1* promoter increased whilst  
319 that of the *LHY* and *CCA1* promoters decreased in response to warm temperature (Fig. S4).  
320 In particular, *TOC1* did not show responses during the morning. Taken together with the  
321 pattern of *PIF4*, these results indicate a negative correlation between ELF3 speckle formation  
322 and ELF3 activity.

323 During the morning, warm temperature decreased ELF3 nuclear abundance (Fig. 8B)  
324 and the bioluminescence signal driven by the *pELF3:ELF3-LUC* transgene (Fig. 8D). During  
325 the afternoon, warm temperature increased both features (Fig. 8B, D). Harvested hypocotyls  
326 also showed elevated nuclear levels of ELF3 at 28°C (Fig. 8E). Conversely, bioluminescence  
327 driven by the *pELF3:LUC* transgene increased only slightly at 28°C (Fig. 8F). These results  
328 suggest a post-transcriptional control of the ELF3 protein levels, which might involve  
329 increased stability within the speckles.

330 As described above (Fig. 4G-H), during the night, the shift from 10 °C to 28 °C did not  
331 increase the number of ELF3 speckles to the levels observed in seedlings already exposed to  
332 28 °C during the day. Actually, the number of speckles decreased during the night in all  
333 temperature conditions (Fig. 8G and I). However, such a decrease does not reflect enhanced  
334 ELF3 activity because a steady drop in ELF3 protein levels accompanied the decrease in  
335 speckles (Fig. 8H and I).

336

### 337 **Hysteresis in *PIF4* promoter activity**

338

339 In all the experiments described above, temperature shifts coincided with end of the day.  
340 However, under natural conditions temperature fluctuations can occur during the photoperiod.

341 We therefore investigated whether the response pattern of the *PIF4* promoter conserved in  
342 the day the behaviour observed during the night. For this purpose, we exposed the seedlings  
343 to 10°C or 28°C and transferred them at ZT= 4h, either from 10°C to warmer temperatures  
344 (15, 20, 25 or 28°C) or from 28°C to cooler temperatures (25, 20, 15 or 10°C), whilst the  
345 controls remained at 10°C or 28°C. We harvested the seedlings 3 hours after the temperature  
346 shift, i.e., still within the photoperiod (ZT= 7h). Fig. 9A shows a memory of the previous  
347 temperature because for most afternoon temperatures (abscissas) warmer morning  
348 temperatures yielded higher *PIF4* promoter activities for most afternoon temperatures  
349 (abscissas). This memory is entirely associated to hysteresis in promoter activity,  
350 demonstrated by a shift in sensitivity in the way up as compared to the way down.

351 We simultaneously analysed the activity of the *HY5* promoter, which remained largely  
352 unresponsive to the temperature shifts in any of the two directions (Fig. 9B). This indicates  
353 that different mechanisms mediate the persistent effects of previous temperature on *PIF4* and  
354 *HY5* nuclear levels. Compared to the *WT*, the analysis of seedlings bearing *pPIF4-LUC* in the  
355 *elf3* mutant background showed a completely distorted pattern of response to temperature  
356 (Fig. 9C). This indicates that the hysteresis pattern depends on *ELF3*. We therefore  
357 investigated the response of *ELF3* itself.

358

### 359 **Hysteresis in *ELF3* speckle formation**

360

361 We then analysed the formation of the *ELF3* speckles in response to increasing or decreasing  
362 temperatures during the day, in the same conditions used to investigate the hysteresis of the  
363 *PIF4* promoter. The seedlings exposed to 28°C showed more speckles than those exposed to  
364 10°C (Fig. 9D). Noteworthy, the response curve showed a strong shift in sensitivity, which  
365 was higher in the way up than in the way down. Therefore, *ELF3* sub-nuclear location showed  
366 in itself the hysteretic pattern. The activity of the *PIF4* promoter strongly correlated with the  
367 number of *ELF3* speckles formed under the same conditions (Fig. 9E), supporting a link  
368 between speckle formation and reduced *ELF3* activity.

369 Compared to 10°C, 28°C did not increase the number of speckles during the first 4 h of  
370 the day (Fig. S5, see also Fig. 8A). Therefore, all the differences observed in Figure 9D  
371 originated during the afternoon (i.e., between 4 and 7h; Fig. S5). This means that the  
372 speckles appear rapidly during the afternoon, but not in the morning (Fig. S5), suggesting that  
373 other components required for their formation of the speckles become available in the

374 afternoon. Furthermore, the additional speckles formed between 4 and 7 h, even in seedlings  
375 exposed to during the first 4 h at 28°C and then transferred to 10°C. This demonstrates that  
376 warmth induction of ELF3 speckle formation persisted in the cold until the additional putative  
377 components of the speckles became available. The persistence of a warmth-induced state of  
378 ELF3 is consistent with the occurrence of hysteresis.

379

## 380 Discussion

381

382 The results reported here demonstrate that the control of hypocotyl growth and gene  
383 expression during the night respond not only to the current temperature environment but also  
384 to the temperature experienced during the preceding photoperiod (Figs 1-2). Therefore, there  
385 is a nighttime memory of daytime temperature.

386 PIF4 and HY5 store daytime temperature information to the control of hypocotyl growth  
387 during the night. First, the genetic analysis of the growth response indicated that the nighttime  
388 memory of daytime temperatures requires HY5 and PIF4 (Fig.3). Second, both HY5 and  
389 PIF4, showed daytime-induced differences in nuclear abundance, which persisted at least 8 h  
390 into the night (Figs 4-5) and correlated with the growth rate during the same period. Third, the  
391 growth memory also required COP1 and ELF3, two signalling components that stored  
392 daytime temperature information (Fig. 4) and control the abundance of HY5 and/or PIF4  
393 (Gangappa and Kumar, 2017; Park et al., 2017; Nusinow et al., 2011; Box et al., 2015). In the  
394 case of PIF4, changes in *PIF4* promoter activity largely accounted for the dynamics of nuclear  
395 protein levels, both during daytime (Fig. 7A-B) and at night (Fig. 6A-B). Apparent post-  
396 transcriptional effects were only transient and changed properly their direction during the  
397 course of the photoperiod (Fig. 6C).

398 One of the features of the nighttime memory of daytime temperatures is the slow  
399 transition in the status of PIF4 and HY5. In the plants shifted from 10°C to 28°C at the  
400 beginning of the night, the nuclear levels of PIF4 and HY5 took 8 h to achieve the levels  
401 observed in the seedlings that were already at the nighttime temperature during the day (Fig.  
402 5A-B). Similarly, in the plants shifted from 28°C to 10°C at the beginning of the night, the  
403 nuclear levels of HY5 took 12 h to reach the levels observed in the seedlings that were  
404 already at this nighttime temperature during the day (Fig. 5B). The slow kinetics of these  
405 responses is intriguing because at least in the case of PIF4 it represents a night-specific  
406 feature. In fact, during the day plants transferred from 10°C to 28°C rapidly (< 3 h) reached

407 the high *PIF4* promoter activity observed in the seedlings already exposed hours earlier to  
408 28°C (Fig. S5). Furthermore, contrary to daytime effects into the night, the differences in  
409 hypocotyl nuclear levels of *PIF4* generated by nighttime temperatures of 10°C compared to  
410 28°C rapidly (<4 h) reverted during the photoperiod (Murcia et al., 2020). This slower  
411 nighttime response of *PIF4* might relate to the gating activity of *TOC1* (Zhu et al., 2016).

412 A second feature of the nighttime memory of daytime temperatures is that in plants  
413 transferred from warm daytime temperatures to cold nights, *PIF4* persisted at the high levels  
414 observed in the plants that remained in the warmth (Fig. 5A). Therefore, there is a clear  
415 asymmetry in the response of *PIF4* to a temperature increase or decrease, with a slow rise of  
416 *PIF4* in the first case and nearly no response in the latter. The *PIF4* target promoter *PIL1* also  
417 showed asymmetric responses, as a change from low to high temperature caused a  
418 significant increase in activity but the opposite modification resulted in a barely any detectable  
419 changes (Fig. 2A). The asymmetric sensitivity of *PIF4* promoter activity was not specific to  
420 changes in temperature during the night. In fact, the response curve to temperature changes  
421 during the afternoon also indicated greater sensitivity in the way up than in the way down (Fig.  
422 9A). This pattern revealed strong hysteresis of *PIF4* promoter activity; i.e., the response to  
423 temperature follows a pattern in the forward direction but a different one in the return direction  
424 (Davies, 2017; Jiang and Hao, 2021).

425 *ELF3* played a fundamental role in the dynamics of *PIF4* promoter activity. Although  
426 during the morning the *PIF4* promoter responded to temperature even in the absence of  
427 *ELF3*, these differences persisted to the beginning of the night and beyond only in the  
428 presence of *ELF3* (Fig. 7B, D). The hysteretic pattern of the *PIF4* promoter activity also  
429 required *ELF3* (Fig. 9C).

430 Warm temperatures reduce evening complex transcriptional activity (Box et al., 2015;  
431 Ezer et al., 2017; Silva et al., 2020) but there is some controversy regarding the response to  
432 temperature of nuclear *ELF3* speckle formation and the function of these sub-nuclear  
433 structures. According to Jung *et al.*, (2020) warm temperatures induce the formation of  
434 speckles containing *ELF3* in root cells but according to Ronald *et al.* (2021), warm  
435 temperatures reduce the formation of speckles in hypocotyl and root cells. Here we show that  
436 both patterns are not mutually exclusive because warm temperature reduced speckle  
437 formation in hypocotyl cells during the morning and increased speckle formation during the  
438 afternoon (Fig. 8A, S5). The cellular context appears therefore to affect *ELF3* speckle  
439 formation. This time of day effect would not be mediated by *ELF4* (Ronald et al., 2021). There

440 is a negative association between ELF3 activity and *PIF4* expression (Nusinow et al., 2011;  
441 Box et al., 2015; Raschke et al., 2015; Press et al., 2016). Under our conditions, ELF3  
442 speckle formation correlated with enhanced *PIF4* promoter activity (Fig. 9F) and hence  
443 reduced ELF3 activity. Membrane-less compartments were linked to changes in the stability  
444 of their components (Kim et al., 2021; Emenecker et al., 2021) and warm temperatures  
445 increased the abundance of ELF3 (Fig. 8B and D) (see also Ding *et al.*, 2018; Zhang *et al.*,  
446 2021). This observation suggests that condensation in speckles protects ELF3 from  
447 degradation, as is the case of phyB in nuclear bodies (Rausenberger et al., 2010; Van Buskirk  
448 et al., 2014).

449 The formation of speckles by ELF3 itself showed hysteresis, as revealed by a  
450 significant shift in the sensitivity to temperature, when this is decreased as compared to when  
451 it is increased (Fig. 9D). Since the pattern of *PIF4* promoter activity requires ELF3 and  
452 correlates with ELF3 speckle formation (Fig. 9A, C, F), we conclude that ELF3 achieves  
453 hysteresis and drives the *PIF4* promoter into the same behaviour. What are the mechanisms  
454 that generate ELF3 hysteresis? Nuclear speckles are condensates, membrane-less  
455 compartments that may be formed by liquid-liquid phase separation (Emenecker et al., 2021).  
456 ELF3 undergoes phase separation to form nuclear speckles under warm temperatures; and  
457 both, *in vitro* phase separation and nuclear speckle formation depend on the intrinsically  
458 disordered prion-like domain of the protein (Jung et al., 2020). Hysteretic phase separation of  
459 intrinsically disordered proteins can emerge from intermolecular interactions that stabilise the  
460 aggregated phase (Quiroz et al., 2019); i.e., the origin of these hysteretic patterns could be at  
461 the ELF3 molecule itself. In fact, in response to increasing temperatures, purified ELF3 prion  
462 domain peptides form liquid droplets *in vitro*, and reversibility by temperature decreases is  
463 shifted towards lower temperatures (Jung et al., 2020), as observed here for *in vivo* speckle  
464 formation (Fig. 9D). Furthermore, ELF3 retained the memory of warm temperatures even  
465 before it formed speckles *in vivo* (Fig. S5). The so-called ‘mnemons’ are proteins that  
466 oligomerise to form condensates and establish long-lasting signalling changes, encoding a  
467 memory of previous conditions (Reichert and Caudron, 2021). There is abundant evidence for  
468 the function of these assemblies in yeast and *Drosophila* (Reichert and Caudron, 2021).

469 In conclusion, the history-dependent behaviour of *PIF4* and *HY5* and their upstream  
470 regulators ELF3 and COP1 enabled a memory of past temperature conditions. Some of these  
471 components, such as *PIF4* and ELF3, drive this memory in one direction, as cooling barely  
472 affected the status established by warmth. Temperature is a variable aspect of the

473 environment and here we show that cues provided by warm days and warm nights operate  
474 synergistically. Thus, integration of temperature information from different phases of the day  
475 has a main role in enabling plants attenuating their response to transitory oscillations in  
476 temperature (Fig. 1A, Table S1A).

477

## 478 **Materials and methods**

479

### 480 **Plant material**

481 We used *Arabidopsis thaliana*. The experiments where we measured hypocotyl growth or  
482 cotyledon expansion included the WT Columbia (Col-0). We list the mutant alleles and  
483 transgenic reporter lines in Table S2.

484

### 485 **Growth conditions**

486 We used clear plastic boxes (4 x 3.5 x 2 cm<sup>3</sup> height) for growth (14 seeds per genotype and  
487 box), microscopy (5 seeds per box) and protein blot (80 seeds per box) and microtiter plates  
488 for bioluminescence experiments (one seed per well). The substrate was 1.5 % agar-water.  
489 After sowing, we incubated the seeds for 4 days at 4 °C in darkness and transferred the  
490 stratified seeds to white light at 90 μmol m<sup>-2</sup> s<sup>-1</sup> (400-700 nm), provided by a mixture of  
491 fluorescent and halogen lamps, with a red/far-red ratio typical of sunlight (1.1), a photoperiod  
492 of 10 h (short day), and 20°C for 4 days. At the beginning of the fourth photoperiod (ZT= 0h),  
493 the seedlings received either white light or simulated shade (9 μmol m<sup>-2</sup> s<sup>-1</sup> between 400 and  
494 700 nm with a red/far-red ratio of 0.1) at 10°C, 20°C or 28°C. For simulated shade, we  
495 combined the white light source with two green acetate filters (LEE filters 089). The seedlings  
496 initiated the night (ZT= 10 h) with or without 10 min of far-red light at 7 μmol m<sup>-2</sup> s<sup>-1</sup> (EOD FR),  
497 provided by 150 W incandescent lamps (R95, Philips) in combination with yellow, orange and  
498 red acetate filters (LEE filters 101, 105 and 106, respectively) and six blue acrylic filters  
499 (Paolini 2031, Buenos Aires, Argentina). Night temperature was 10°C, 20°C or 28°C. To  
500 investigate the occurrence of hysteresis without involving a light-to-dark transition, in some  
501 experiments, 4 h after the beginning of the fourth photoperiod (ZT= 4h), we introduced  
502 temperature shifts while the plants remained under white light.

503

504

505



## 506 **Hypocotyl growth rate**

507 We photographed the seedlings with a digital camera (PowerShot; Canon, Tokyo, Japan) at  
508 the beginning of the night (ZT= 10 h) of the fourth photoperiod and either at the end of the  
509 night (ZT= 24 h) or at intermediate times (ZT= 14 h, 18 h and 22 h). We measured hypocotyl  
510 length increments by using an image processing software as described (Legris et al., 2016).

## 512 **Bioluminescence**

513 We detected luciferase (LUC) activity with a Centro LB 960 (Berthold) luminometer by adding  
514 20  $\mu$ L of 0.2 mM D-luciferin per well 24 h before starting the measurements.

## 516 **Confocal microscopy**

517 We obtained confocal fluorescence images from the epidermis and the first sub-epidermal  
518 layers of either the upper third portion of the hypocotyl (PIF4, HY5 and COP1) or individual  
519 nuclei present in the same region (ELF3) with a LSM5 Pascal laser-scanning microscope  
520 (Zeiss). The water-immersion objective lens were C-Apochromat X40/1.2 or C-Apochromatic  
521 X63/1.2 (Zeiss), respectively. We used an argon laser ( $\lambda$ = 488 nm) for excitation of GFP or  
522 YFP and a BP 505-530 filter for detection of fluorescence. We used a He-Ne laser ( $\lambda$  = 543  
523 nm) for excitation of chlorophyll and a LP 560 filter for detection of its fluorescence and  
524 configured a transmitted light channel to visualise cellular structures. We performed image  
525 analysis in batch with an image segmentation program developed in Icy  
526 (<http://icy.bioimageanalysis.org/>) (Sellaro et al., 2019).

## 528 **Protein blots**

529 We extracted total protein from 100 mg of seedlings by homogenizing plant material in  
530 extraction buffer containing 50 mM Tris-HCl (pH 7.5), 200 mM NaCl, 10 % (v/v) glycerol, 0.1  
531 % (v/v) Tween-20, 1 mM PMSF and protease inhibitors (Roche), centrifuged twice (20 000 *g*,  
532 15 min, at 4 °C), and transferred the supernatant into fresh Eppendorf reaction tubes. The  
533 protein concentration in the supernatant was determined by the Bradford assay (Bio-Rad).  
534 Protein samples were boiled (95 °C, 5 min) in TMx4 loading buffer. We run 20  $\mu$ g of protein in  
535 8% SDS-PAGE followed by wet blotting (100 mM Tris/Glycine, 10 % MeOH, 1.5 h).  
536 Homogeneous protein transfer to nitrocellulose membranes (Whatman) was confirmed by  
537 Ponceau red staining. Membranes were blocked (5 % milk powder, 0.1 % Tween-20 in TBS,  
538 2 h) and incubated with primary antibody (anti-HA, 1:1000, Sigma) overnight, followed by

539 incubation with anti-rabbit HRP-conjugated antibody (1:5000, Sigma) during 2 h. For  
540 35S:PIF4-HA we used an anti-HA Peroxidase (Roche) antibody. We used ImageJ for  
541 quantification of the bands.

542

543

544

## 545 **Supplemental data**

546 The following materials are available in the online version of this article

547 **Supplemental Figure S1.** Effects of daytime temperature on nighttime growth in  
548 multiple *pif* mutants.

549 **Supplemental Figure S2.** Daytime temperature affects nuclear fluorescence driven by  
550 the *pPIF4:PIF4-GFP* transgene in the cotyledons.

551 **Supplemental Figure S3.** Warm temperatures post-transcriptionally enhance PIF4  
552 abundance.

553 **Supplemental Figure S4.** Temperature effects on the time course of *TOC1*, *LHY* and  
554 *CCA1* promoter activities.

555 **Supplemental Table S1.** Detailed statistical analysis of the data.

556 **Supplemental Table S2.** Mutant and transgenic lines used in this study.

557

## 558 **Acknowledgments**

559 The authors are grateful to Dr Christian Fankhauser (University of Lausanne) for providing  
560 seed samples of the lines *pPIF7:PIF7-3HA-tPIF7* and *p35S:PIF4-HA*.

561

562

## 563 **Funding**

564 This work was supported by the Argentinian *Agencia Nacional de Promoción Científica y*  
565 *Tecnológica* (grants PICT-2016-1459 and PICT-2018-01695 to JJC), *Universidad de Buenos*  
566 *Aires* (grant 20020170100505BA to JJC) and the Spanish *Ministerio de Ciencia e Innovación*  
567 (grant BIO2017-90056-R to SP).

568

569 *Conflict of interest statement.* None declared

570

571 GM and JJC conceived and designed the experiments. SP and CN provided insightful  
572 suggestions. GM, CN and RS performed the experiments. SP provided new reporter lines.  
573 GM, CN, RS, SP and JJC analysed the data. GM and JJC wrote the paper with input from the  
574 other authors.

575

576

## 577 **References**

578

579 **Anwer, M.U., Davis, A., Davis, S.J., and Quint, M.** (2020). Photoperiod sensing of the  
580 circadian clock is controlled by EARLY FLOWERING 3 and GIGANTEA. *Plant J.* **101**:  
581 1397–1410.

582 **Bellstaedt, J., Trenner, J., Lippmann, R., Poeschl, Y., Zhang, X., Friml, J., Quint, M., and**  
583 **Delker, C.** (2019). A mobile auxin signal connects temperature sensing in cotyledons  
584 with growth responses in hypocotyls. *Plant Physiol.* **180**: 757–766.

585 **Bours, R., Kohlen, W., Bouwmeester, H.J., and van der Krol, A.** (2015). Thermoperiodic  
586 control of hypocotyl elongation depends on auxin-induced ethylene signaling that controls  
587 downstream PHYTOCHROME INTERACTING FACTOR3 activity. *Plant Physiol.* **167**:  
588 517–30.

589 **Bours, R., van Zanten, M., Pierik, R., Bouwmeester, H., and van der Krol, A.** (2013).  
590 Antiphase light and temperature cycles affect PHYTOCHROME B-controlled ethylene  
591 sensitivity and biosynthesis, limiting leaf movement and growth of Arabidopsis. *Plant*  
592 *Physiol.* **163**: 882–95.

593 **Box, M.S. et al.** (2015). ELF3 controls thermoresponsive growth in Arabidopsis. *Curr. Biol.*  
594 **25**: 194–199.

595 **Burgie, E.S., Gannam, Z.T.K., McLoughlin, K.E., Sherman, C.D., Holehouse, A.S.,**  
596 **Stankey, R.J., and Vierstra, R.D.** (2021). Differing biophysical properties underpin the  
597 unique signaling potentials within the plant phytochrome photoreceptor families. *Proc.*  
598 *Natl. Acad. Sci.* **118**: e2105649118.

599 **Van Buskirk, E.K., Reddy, A.K., Nagatani, A., and Chen, M.** (2014). Photobody localization  
600 of phytochrome B is tightly correlated with prolonged and light-dependent inhibition of  
601 hypocotyl elongation in the dark. *Plant Physiol.* **165**: 595–607.

602 **Casal, J.J. and Balasubramanian, S.** (2019). Thermomorphogenesis. *Annu. Rev. Plant Biol.*  
603 **70**: 321–346.

- 604 **Catalá, R., Medina, J., and Salinas, J.** (2011). Integration of low temperature and light  
605 signaling during cold acclimation response in Arabidopsis. *Proc. Natl. Acad. Sci. U. S. A.*  
606 **108**: 16475–16480.
- 607 **Cheng, M.-C., Kathare, P.K., Paik, I., and Huq, E.** (2021). Phytochrome Signaling Networks.  
608 *Annu. Rev. Plant Biol.* **72**: 217–244.
- 609 **Chung, B.Y.W., Balcerowicz, M., Di Antonio, M., Jaeger, K.E., Geng, F., Franaszek, K.,**  
610 **Marriott, P., Brierley, I., Firth, A.E., and Wigge, P.A.** (2020). An RNA thermoswitch  
611 regulates daytime growth in Arabidopsis. *Nat. Plants* **6**: 522–532.
- 612 **Crawford, A.J., McLachlan, D.H., Hetherington, A.M., and Franklin, K.A.** (2012). High  
613 temperature exposure increases plant cooling capacity. *Curr. Biol.* **22**: R396-7.
- 614 **Davies, J.** (2017). Using synthetic biology to explore principles of development. *Dev.* **144**:  
615 1146–1158.
- 616 **Delker, C. et al.** (2014). The DET1-COP1-HY5 pathway constitutes a multipurpose signaling  
617 module regulating plant photomorphogenesis and thermomorphogenesis. *Cell Rep.* **9**:  
618 1983–1989.
- 619 **Ding, L., Wang, S., Song, Z.T., Jiang, Y., Han, J.J., Lu, S.J., Li, L., and Liu, J.X.** (2018).  
620 Two B-Box Domain Proteins, BBX18 and BBX23, Interact with ELF3 and Regulate  
621 Thermomorphogenesis in Arabidopsis. *Cell Rep.* **25**: 1718-1728.e4.
- 622 **Emenecker, R.J., Holehouse, A.S., and Strader, L.C.** (2021). Biological Phase Separation  
623 and Biomolecular Condensates in Plants. *Annu. Rev. Plant Biol.* **72**: 17–46.
- 624 **Ezer, D. et al.** (2017). The evening complex coordinates environmental and endogenous  
625 signals in Arabidopsis. *Nat. Plants* **3**: 17087.
- 626 **Fehér, B., Kozma-Bognár, L., Kevei, É., Hajdu, A., Binkert, M., Davis, S.J., Schäfer, E.,**  
627 **Ulm, R., and Nagy, F.** (2011). Functional interaction of the circadian clock and UV  
628 RESISTANCE LOCUS 8-controlled UV-B signaling pathways in Arabidopsis thaliana.  
629 *Plant J.* **67**: 37–48.
- 630 **Fiorucci, A.-S., Galvão, V.C., Ince, Y.Ç., Boccaccini, A., Goyal, A., Allenbach Petrolati,**  
631 **L., Trevisan, M., and Fankhauser, C.** (2020). PHYTOCHROME INTERACTING  
632 FACTOR 7 is important for early responses to elevated temperature in Arabidopsis  
633 seedlings. *New Phytol.* **226**: 50–58.
- 634 **Foreman, J., Johansson, H., Hornitschek, P., Josse, E.-M.M., Fankhauser, C., and**  
635 **Halliday, K.J.** (2011). Light receptor action is critical for maintaining plant biomass at  
636 warm ambient temperatures. *Plant J.* **65**: 441–452.

- 637 **Gangappa, S.N. and Kumar, S.V.** (2017). DET1 and HY5 Control PIF4-Mediated  
638 Thermosensory Elongation Growth through Distinct Mechanisms. *Cell Rep.* **18**: 344–351.
- 639 **Gray, W.M., Östin, A., Sandberg, G., Romano, C.P., and Estelle, M.** (1998). High  
640 temperature promotes auxin-mediated hypocotyl elongation in Arabidopsis. *Proc. Natl.*  
641 *Acad. Sci. U. S. A.* **95**: 7197–7202.
- 642 **Herrero, E. et al.** (2012). EARLY FLOWERING4 recruitment of EARLY FLOWERING3 in the  
643 nucleus sustains the Arabidopsis circadian clock. *Plant Cell* **24**: 428–43.
- 644 **Hornitschek, P., Lorrain, S., Zoete, V., Michielin, O., and Fankhauser, C.** (2009). Inhibition  
645 of the shade avoidance response by formation of non-DNA binding bHLH heterodimers.  
646 *EMBO J.* **28**: 3893–3902.
- 647 **Huq, E. and Quail, P.** (2002). PIF4, a phytochrome-interacting bHLH factor, functions as a  
648 negative regulator of phytochrome B signaling in Arabidopsis. *EMBO J.* **21**: 2441–2450.
- 649 **Jiang, Y. and Hao, N.** (2021). Memorizing environmental signals through feedback and  
650 feedforward loops. *Curr. Opin. Cell Biol.* **69**: 96–102.
- 651 **Jung, J.-H. et al.** (2016). Phytochromes function as thermosensors in Arabidopsis. *Science*  
652 (80-. ). **354**: 886–889.
- 653 **Jung, J.H. et al.** (2020). A prion-like domain in ELF3 functions as a thermosensor in  
654 Arabidopsis. *Nature* **585**: 256–260.
- 655 **Kim, J., Lee, H., Lee, H.G., and Seo, P.J.** (2021). Get closer and make hotspots: liquid–  
656 liquid phase separation in plants. *EMBO Rep.* **22**: 1–15.
- 657 **Koini, M.A., Alvey, L., Allen, T., Tilley, C. a, Harberd, N.P., Whitelam, G.C., and Franklin,**  
658 **K. a** (2009). High temperature-mediated adaptations in plant architecture require the  
659 bHLH transcription factor PIF4. *Curr. Biol.* **19**: 408–13.
- 660 **Legris, M., Klose, C., Burgie, E., Costigliolo Rojas, C., Neme, M., Hiltbrunner, A.,**  
661 **Wigge, P.A., Schäfer, E., Vierstra, R.D., and Casal, J.J.** (2016). Phytochrome B  
662 integrates light and temperature signals in Arabidopsis. *Science* (80-. ). **354**: 897–900.
- 663 **Legris, M., Nieto, C., Sellaro, R., Prat, S., and Casal, J.J.** (2017). Perception and signalling  
664 of light and temperature cues in plants. *Plant J.* **90**: 683–697.
- 665 **Murcia, G., Enderle, B., Hiltbrunner, A., and Casal, J.J.** (2020). Phytochrome B and PCH1  
666 protein dynamics store night temperature information. *Plant J.*: in press.
- 667 **Nieto, C., López-Salmerón, V., Davière, J.-M., and Prat, S.** (2015). ELF3-PIF4 interaction  
668 regulates plant growth independently of the Evening Complex. *Curr. Biol.* **25**: 187–93.
- 669 **Nusinow, D. a, Helfer, A., Hamilton, E.E., King, J.J., Imaizumi, T., Schultz, T.F., Farré,**

- 670 **E.M., and Kay, S. a** (2011). The ELF4-ELF3-LUX complex links the circadian clock to  
671 diurnal control of hypocotyl growth. *Nature* **475**: 398–402.
- 672 **Park, Y.-J., Lee, H.-J., Ha, J.-H., Kim, J.Y., and Park, C.-M.** (2017). COP1 conveys warm  
673 temperature information to hypocotyl thermomorphogenesis. *New Phytol.* **215**: 269–280.
- 674 **Press, M.O., Lanctot, A., and Queitsch, C.** (2016). PIF4 and ELF3 act independently in  
675 *Arabidopsis thaliana* thermoresponsive flowering. *PLoS One* **11**: 14–16.
- 676 **Quint, M., Delker, C., Franklin, K.A., Wigge, P.A., Halliday, K.J., and van Zanten, M.**  
677 (2016). Molecular and genetic control of plant thermomorphogenesis. *Nat. Plants* **2**:  
678 15190.
- 679 **Quiroz, F.G., Li, N.K., Roberts, S., Weber, P., Dzuricky, M., Weitzhandler, I., Yingling,**  
680 **Y.G., and Chilkoti, A.** (2019). Intrinsically disordered proteins access a range of  
681 hysteretic phase separation behaviors. *Sci. Adv.* **5**: 1–12.
- 682 **Raschke, A. et al.** (2015). Natural variants of ELF3 affect thermomorphogenesis by  
683 transcriptionally modulating PIF4-dependent auxin responses. *BMC Plant Biol.* **15**: 197.
- 684 **Rausenberger, J., Hussong, A., Kircher, S., Kirchenbauer, D., Timmer, J., Nagy, F.,**  
685 **Schäfer, E., and Fleck, C.** (2010). An integrative model for phytochrome B mediated  
686 photomorphogenesis: from protein dynamics to physiology. *PLoS One* **5**: :e10721.
- 687 **Reichert, P. and Caudron, F.** (2021). Mnemons and the memorization of past signaling  
688 events. *Curr. Opin. Cell Biol.* **69**: 127–135.
- 689 **Romero-Montepaone, S., Sellaro, R., Hernando, C.E., Costigliolo-Rojas, C.,**  
690 **Bianchimano, L., Ploschuk, E.L., Yanovsky, M.J., and Casal, J.J.** (2021). Functional  
691 convergence of growth responses to shade and warmth in *Arabidopsis*. *New Phytol.*:  
692 [doi.org/10.1111/nph.17430](https://doi.org/10.1111/nph.17430).
- 693 **Ronald, J., Wilkinson, A.J., and Davis, S.J.** (2021). EARLY FLOWERING3 sub-nuclear  
694 localization responds to changes in ambient temperature. *Plant Physiol.*: 1–4.
- 695 **Sandi Paulišić, Qin, W., Harshul Arora Verasztó, C.T., Nogue, B., Alary, F., Tsiantis, M.,**  
696 **Hothorn, M., and Martínez-García, J.F.** (2021). Adjustment of the PIF7-HFR1  
697 transcriptional module activity controls plant shade adaptation. *EMBO J.* **40**: e104273.
- 698 **Sellaro, R., Smith, R.W., Legris, M., Fleck, C., and Casal, J.J.** (2019). Phytochrome B  
699 dynamics departs from photoequilibrium in the field. *Plant. Cell Environ.* **42**: 606–617.
- 700 **Silva, C.S., Nayak, A., Lai, X., Hutin, S., Hugouvieux, V., Jung, J.-H., López-Vidriero, I.,**  
701 **Franco-Zorrilla, J.M., Panigrahi, K.C.S., Nanao, M.H., Wigge, P.A., and Zubieta, C.**  
702 (2020). Molecular mechanisms of Evening Complex activity in *Arabidopsis*. *Proc. Natl.*

703 Acad. Sci. U. S. A. **117**: 6901–6909.

704 **Stavang, J.A., Gallego-Bartolomé, J., Gómez, M.D., Yoshida, S., Asami, T., Olsen, J.E.,**  
705 **García-Martínez, J.L., Alabadí, D., and Blázquez, M.A.** (2009). Hormonal regulation of  
706 temperature-induced growth in Arabidopsis. *Plant J.* **60**: 589–601.

707 **Sun, J., Qi, L., Li, Y., Chu, J., and Li, C.** (2012). PIF4-mediated activation of YUCCA8  
708 expression integrates temperature into the auxin pathway in regulating arabidopsis  
709 hypocotyl growth. *PLoS Genet.* **8**: e1002594.

710 **Thines, B. and Harmon, F.G.** (2010). Ambient temperature response establishes ELF3 as a  
711 required component of the core Arabidopsis circadian clock. *Proc. Natl. Acad. Sci. U. S.*  
712 *A.* **107**: 3257–3262.

713 **Toledo-Ortiz, G., Johansson, H., Lee, K.P., Bou-Torrent, J., Stewart, K., Steel, G.,**  
714 **Rodríguez-Concepción, M., and Halliday, K.J.** (2014). The HY5-PIF regulatory module  
715 coordinates light and temperature control of photosynthetic gene transcription. *PLoS*  
716 *Genet.* **10**: e1004416.

717 **Zhang, L.L., Li, W., Tian, Y.Y., Davis, S.J., and Liu, J.X.** (2021). The E3 ligase XBAT35  
718 mediates thermoresponsive hypocotyl growth by targeting ELF3 for degradation in  
719 Arabidopsis. *J. Integr. Plant Biol.* **63**: 1097–1103.

720 **Zhu, J.-Y., Oh, E., Wang, T., and Wang, Z.-Y.** (2016). TOC1–PIF4 interaction mediates the  
721 circadian gating of thermoresponsive growth in Arabidopsis. *Nat. Commun.* **7**: 13692.

722

723

724 **Legends of the figures**

725  
726 **Figure 1.** Daytime temperatures affect nighttime hypocotyl growth.

727 **(A)** Hypocotyl growth rate measured in Col-0 seedlings during the night (ZT 10h to ZT 24h).  
728 The seedlings received all possible combinations of temperature during the preceding  
729 photoperiod (10, 20 or 28°C), nighttime temperature (10, 20 or 28°C), daytime light (upper  
730 panel) or daytime shade (lower panel) and either control or end-of-day far-red treatment (EOD  
731 FR). The left- and right-hand side of the symbols indicate daytime and nighttime  
732 temperatures, respectively. Box plots show median, interquartile range 1-3 and the maximum-  
733 minimum interval of 4 biological replicates (see Table S1A for detailed statistics).

734 **(B)** Hypocotyl length increment measured in Col-0 seedlings during the night (starting at ZT=  
735 10h) as affected by four combinations of daytime temperature (10 or 28°C) and nighttime  
736 temperature (10 or 28°C). All seedlings received shade during the day and EOD FR. Data are  
737 means  $\pm$  SE of nine biological replicates for each time point. The interaction between  
738 nighttime and daytime temperatures persists beyond ZT= 14 (see Table S1B for detailed  
739 statistics).

740  
741 **Figure 2.** Daytime temperatures affect nighttime gene expression.

742 **(A)** and **(B)** Time course of luciferase activity driven by the *pPIL1:LUC* (A) or *pIAA19:LUC* (B).  
743 Luminescence was recorded during the night (starting at ZT= 10h) as affected by four  
744 combinations of daytime temperature (10 or 28°C) and nighttime temperature (10 or 28°C). All  
745 seedlings received shade during the day and EOD FR. Data are means  $\pm$  SE of three plates  
746 with 96 seedlings (see Tables S1C-D for detailed statistics).

747  
748 **Figure 3.** Genetic requirements of the effects of daytime temperature on nighttime growth.

749 **(A)** and **(C)** Hypocotyl growth rate measured in seedlings of the indicated genotypes during  
750 the night (ZT 10h to ZT 24h) as affected by two different daytime temperatures (10 or 28°C).  
751 **(B)** and **(D)** Slope of the responses to daytime temperature (linear regression analysis of the  
752 data in A and C, respectively).

753 All seedlings received shade during the day and EOD FR. Night temperature was 28°C (A-B)  
754 or 10°C (C-D). Box plots show median, interquartile range 1-3 and the maximum-minimum  
755 interval of 8-12 biological replicates (see Table S1 E-F for detailed statistics). In B and D, the  
756 asterisks indicate significant differences with Col-0 according to *t*-tests (\*,  $p < 0.05$ ).



757

758 **Figure 4.** Daytime temperatures affect nighttime signalling status.

759 **(A-B)** Nuclear fluorescence driven in hypocotyl cells by *p35S:YFP-COP1*.

760 **(C-D)** Nuclear fluorescence driven in hypocotyl cells by *pHY5:HY5-YFP*.

761 **(E-F)** Nuclear fluorescence driven in hypocotyl cells by *pPIF4:PIF4-GFP*.

762 **(G-H)** Number of ELF3 nuclear speckles (square root-transformed data) in the hypocotyl cells  
763 of the line expressing the *p35S:YFP-ELF3* transgene.

764 **(I-J)** Abundance of PIF7 in seedlings bearing *pPIF7:PIF7-HA*.

765 **(K-L)** Luciferase activity driven by *pHFR1:LUC* (K) or *p35S:HFR1-LUC* (L).

766 The seedlings received shade and either 10°C or 28°C during the day, EOD FR and 28°C  
767 during the night. Box plots show median, interquartile range 1-3 and the maximum-minimum  
768 interval of 6 (A, C and E), 16 (G), 12 (I), 25 (K), 4 (L) biological replicates. Representative  
769 confocal (B, D, F, H) or protein blot (J) images. Scale bar = 35 µm (B, D, F) and 2.61 µm (H).  
770 Asterisks indicate significant differences in *t*-tests (\*,  $p < 0.05$ ; \*\*,  $p < 0.01$ ; \*\*\*,  $p < 0.001$ ).

771

772 **Figure 5.** Daytime temperature affects nuclear levels of PIF4 and HY5 during the night.

773 **(A-D)** Nighttime kinetics of nuclear fluorescence intensity driven in hypocotyl cells by  
774 *pPIF4:PIF4-GFP* (A-B) or *pHY5:HY5-YFP* (C-D).

775 **(E)** Nighttime kinetics of luminescence driven by *pPIF4:PIF4-LUC* in entire seedlings.

776 **(F)** Luminescence driven by *pPIF4:PIF4-LUC* in isolated hypocotyls harvested at ZT= 14 h.  
777 Confocal images or luminescence values were recorded during the night (starting at ZT= 10h)  
778 as affected by four combinations of daytime temperature and nighttime temperature. All  
779 seedling received shade during the day and EOD FR. (A, C, E) Data are means  $\pm$  SE of three  
780 biological replicates. (F) Box plots show median, interquartile range 1-3 and the maximum-  
781 minimum interval of 10-14 biological replicates. (B, D) Representative confocal images at ZT=  
782 14h. Scale bar = 35 µm. See Table S1G-I for detailed statistics of (A, C, E). In (F), the  
783 asterisks indicates significant differences in *t*-test (\*\*,  $p < 0.01$ ).

784

785 **Figure 6.** Changes in PIF4 promoter activity account for nighttime PIF4 protein dynamics.

786 **(A)** Nighttime kinetics of luminescence driven by *pPIF4:LUC* in entire seedlings.

787 Luminescence was recorded during the night (starting at ZT= 10h) as affected by four  
788 combinations of daytime temperature (10 or 28°C) and nighttime temperature (10 or 28°C). All

789 seedling received shade during the day and EOD FR. Data are means  $\pm$  SE of three plates  
790 with seedlings. See Table S1J-K for detailed statistics.

791 **(B)** Correlation between luminescence driven by *pPIF4:PIF4-LUC* (from 5E) and *pPIF4:LUC*  
792 (from A) in the Col-0 background. The correlation is significant at  $P < 0.0001$ .

793

794

795 **Figure 7.** Temperature effects on end-of-day *PIF4* promoter activity and *PIF4* protein  
796 abundance require *ELF3*.

797 **(A-B)** Time course of daytime luciferase activity driven by *pPIF4:PIF4-LUC* (A) or *pPIF4:LUC*  
798 (B) in the Col-0 and *elf3-8* background, as affected by 10°C or 28°C.

799 **(C)** Ratio between the luciferase signals driven by *pPIF4:PIF4-LUC* and *pPIF4:LUC*.

800 **(D)** Luminescence driven by *pPIF4:LUC* in isolated hypocotyls harvested from Col-0 and *elf3-*  
801 *8* seedlings at ZT= 14 h.

802 All seedling received shade during the day and EOD FR. (A-B) Data are means  $\pm$  SE of 3  
803 plates with seedlings. (D) Box plots show median, interquartile range 1-3 and the maximum-  
804 minimum interval of 24-30 biological replicates, asterisk indicates significant differences in *t*-  
805 tests (\*,  $p < 0.05$ ). See Table S1L-M for detailed statistics of (A-B).

806

807 **Figure 8.** *ELF3* dynamics under contrasting temperatures.

808 **(A-C)** Number of *ELF3* nuclear speckles (A), nuclear fluorescence intensity (B) and  
809 representative confocal images (C) from hypocotyl cells of seedlings expressing *p35S:YFP-*  
810 *ELF3*.

811 **(D)** Luciferase activity driven by *pELF3:ELF3-LUC* in entire seedlings.

812 **(E)** Luciferase activity driven by *pELF3:ELF3-LUC* in isolated hypocotyls.

813 **(F)** Luciferase activity driven by *pELF3:LUC* in entire seedlings.

814 **(G-I)** Number of *ELF3* nuclear speckles (square root-transformed data, G), nuclear  
815 fluorescence intensity (H) and representative confocal images (I) from hypocotyl cells of  
816 seedlings expressing *p35S:YFP-ELF3*.

817 All seedling received shade during the day and EOD FR. (A-B and G-H) Data are means  $\pm$   
818 SE of 20 biological replicates. (C and I) Representative confocal images. Scale bar = 2.61  
819  $\mu\text{m}$ . (D and F) Data are means  $\pm$  SE of three plates with seedlings. (E) Box plots show  
820 median, interquartile range 1-3 and the maximum-minimum interval of 15 biological replicates.

821 See Table S1N-S for detailed statistics of (A-B, D, F-H). In E, asterisks indicate significant  
822 differences in *t*-test (\*\*\*,  $p < 0.001$ ).

823

824 **Figure 9.** Hysteresis of ELF3 drives hysteresis in *PIF4* promoter activity.

825 **(A-C)** Response of the luminescence driven by *pPIF4:LUC* (A and C) or *pPHY5:LUC* (B) in the  
826 Col-0 (A-B) or *elf3* (C) backgrounds to increasing or decreasing temperature.

827 **(D-E)** Response of the number of ELF3 nuclear speckles (square root-transformed data) from  
828 hypocotyl cells of seedlings expressing *p35S:YFP-ELF3* to increasing or decreasing  
829 temperature.

830 **(F)** Correlation between luminescence driven by *pPIF4:LUC* (from A) and the number of  
831 speckles driven by *p35S:YFP-ELF3* (from D).

832 The seedlings were exposed to white light at either 10°C or 28°C and 4 h after the beginning  
833 of the photoperiod were transferred to the temperature indicated in abscissas (including  
834 controls that remained at 10°C or 28°C). Luminescence (A-C) or confocal images (D and E)  
835 were taken 3 h later. Data are means  $\pm$  SE of 3 plates with seedlings (A-C) or 15 biological  
836 replicates (D and E). (E) Representative confocal images. Scale bar = 2.61  $\mu$ m. In F, the  
837 correlation is significant at  $P = 0.0002$ . See Table S1T-X for detailed statistics.

838

839

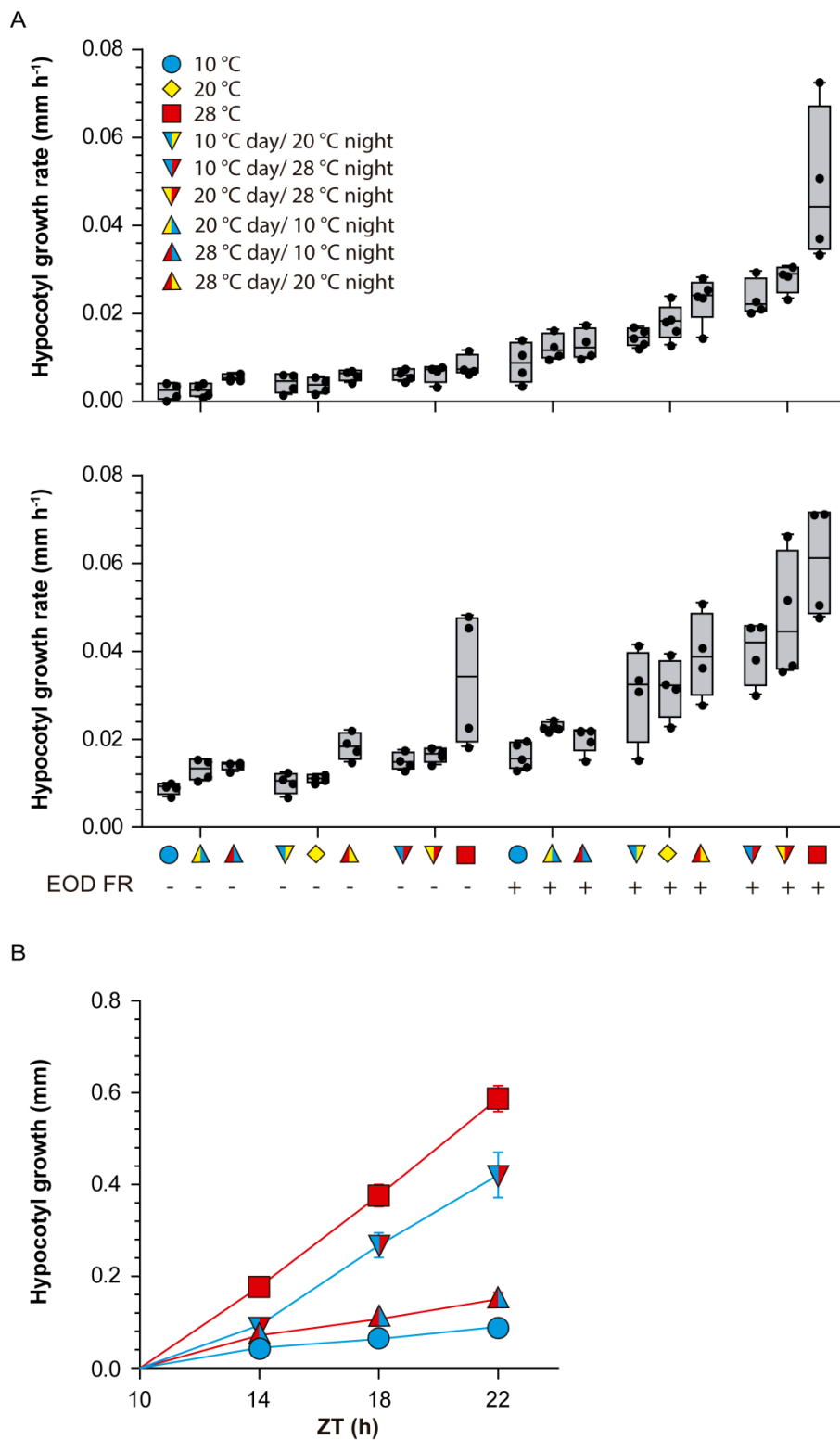


**Figure 1.** Daytime temperatures affect nighttime hypocotyl growth.

**(A)** Hypocotyl growth rate measured in Col-0 seedlings during the night (ZT 10h to ZT 24h). The seedlings received all possible combinations of temperature during the preceding photoperiod (10, 20 or 28°C), nighttime temperature (10, 20 or 28°C), daytime light (upper panel) or daytime shade (lower panel) and either control or end-of-day far-red treatment (EOD FR). The left- and right-hand side of the symbols indicate daytime and nighttime temperatures, respectively. Box plots show median, interquartile range 1-3 and the maximum-minimum interval of 4 biological replicates (see Table S1A for detailed statistics).

**(B)** Hypocotyl length increment measured in Col-0 seedlings during the night (starting at ZT= 10h) as affected by four combinations of daytime temperature (10 or 28°C) and nighttime temperature (10 or 28°C). All seedlings received shade during the day and EOD FR. Data are means  $\pm$  SE of nine biological replicates for each time point. The interaction between nighttime and daytime temperatures persists beyond ZT= 14 (see Table S1B for detailed statistics).

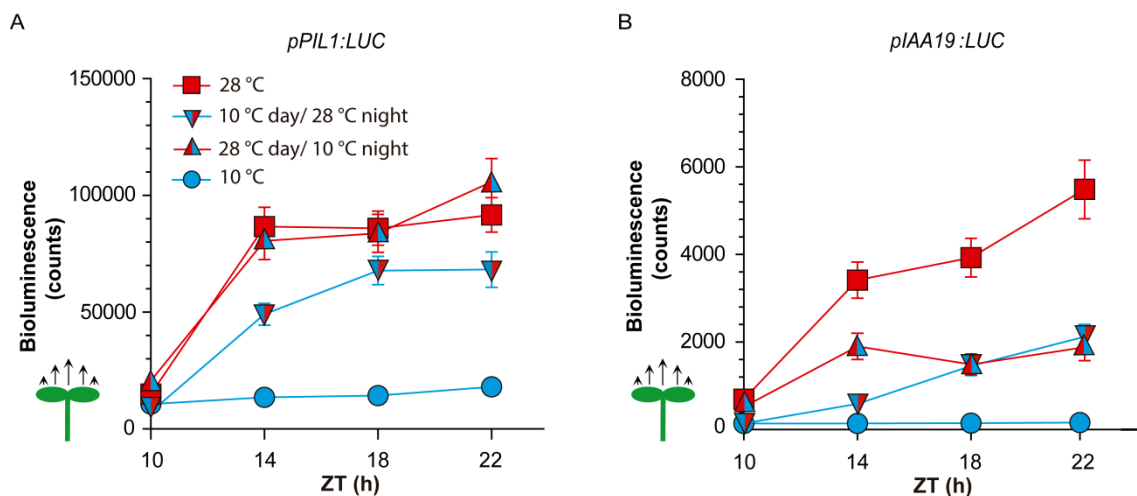


**Figure 2.** Daytime temperatures affect nighttime gene expression.

**(A)** and **(B)** Time course of luciferase activity driven by the *pPIL1:LUC* (A) or *pIAA19:LUC* (B). Luminescence was recorded during the night (starting at ZT= 10h) as affected by four combinations of daytime temperature (10 or 28°C) and nighttime temperature (10 or 28°C). All seedlings received shade during the day and EOD FR. Data are means  $\pm$  SE of three plates with 96 seedlings (see Tables S1C-D for detailed statistics).

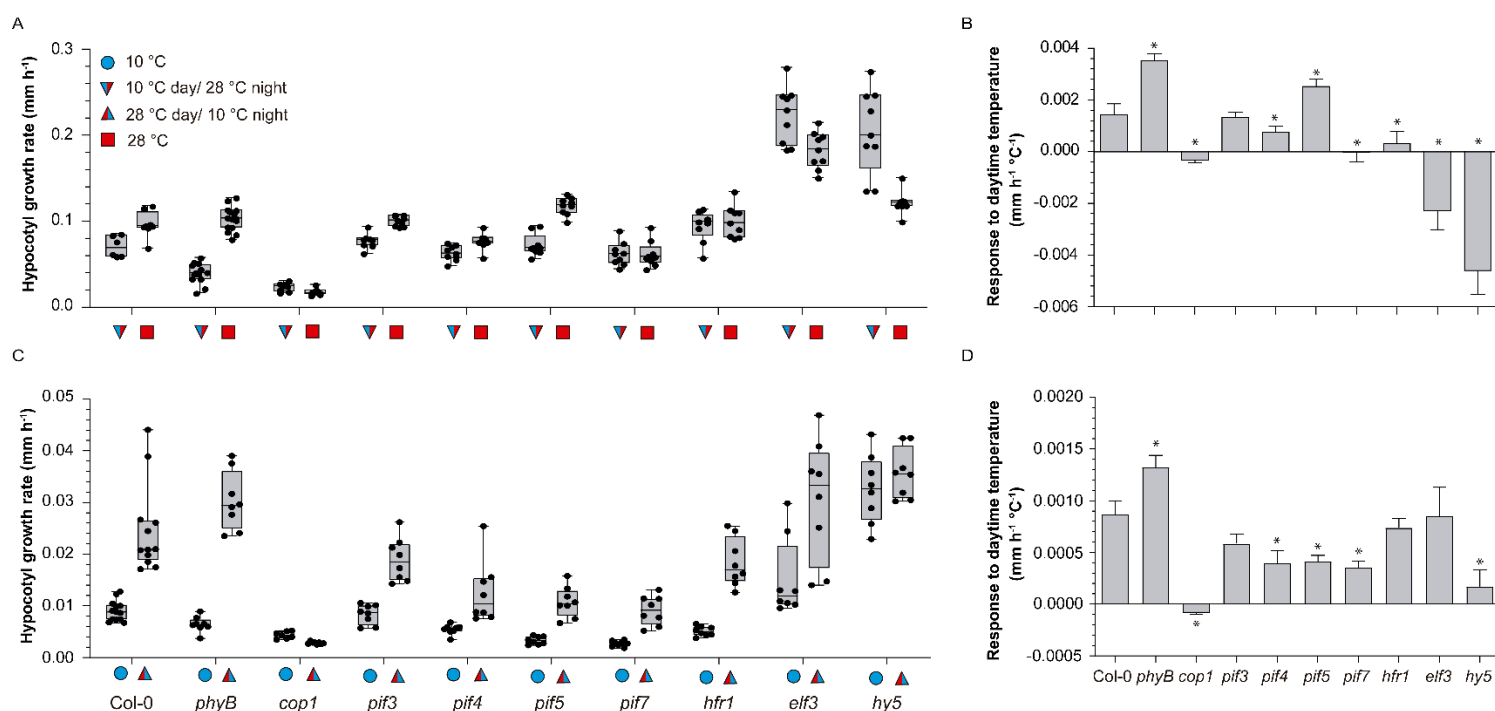


**Figure 3.** Genetic requirements of the effects of daytime temperature on nighttime growth.

**(A)** and **(C)** Hypocotyl growth rate measured in seedlings of the indicated genotypes during the night (ZT 10h to ZT 24h) as affected by two different daytime temperatures (10 or 28°C).

**(B)** and **(D)** Slope of the responses to daytime temperature (linear regression analysis of the data in A and C, respectively).

All seedlings received shade during the day and EOD FR. Night temperature was 28°C (A-B) or 10°C (C-D). Box plots show median, interquartile range 1-3 and the maximum-minimum interval of 8-12 biological replicates (see Table S1 E-F for detailed statistics). In B and D, the asterisks indicate significant differences with Col-0 according to *t*-tests (\*, *p* < 0.05).

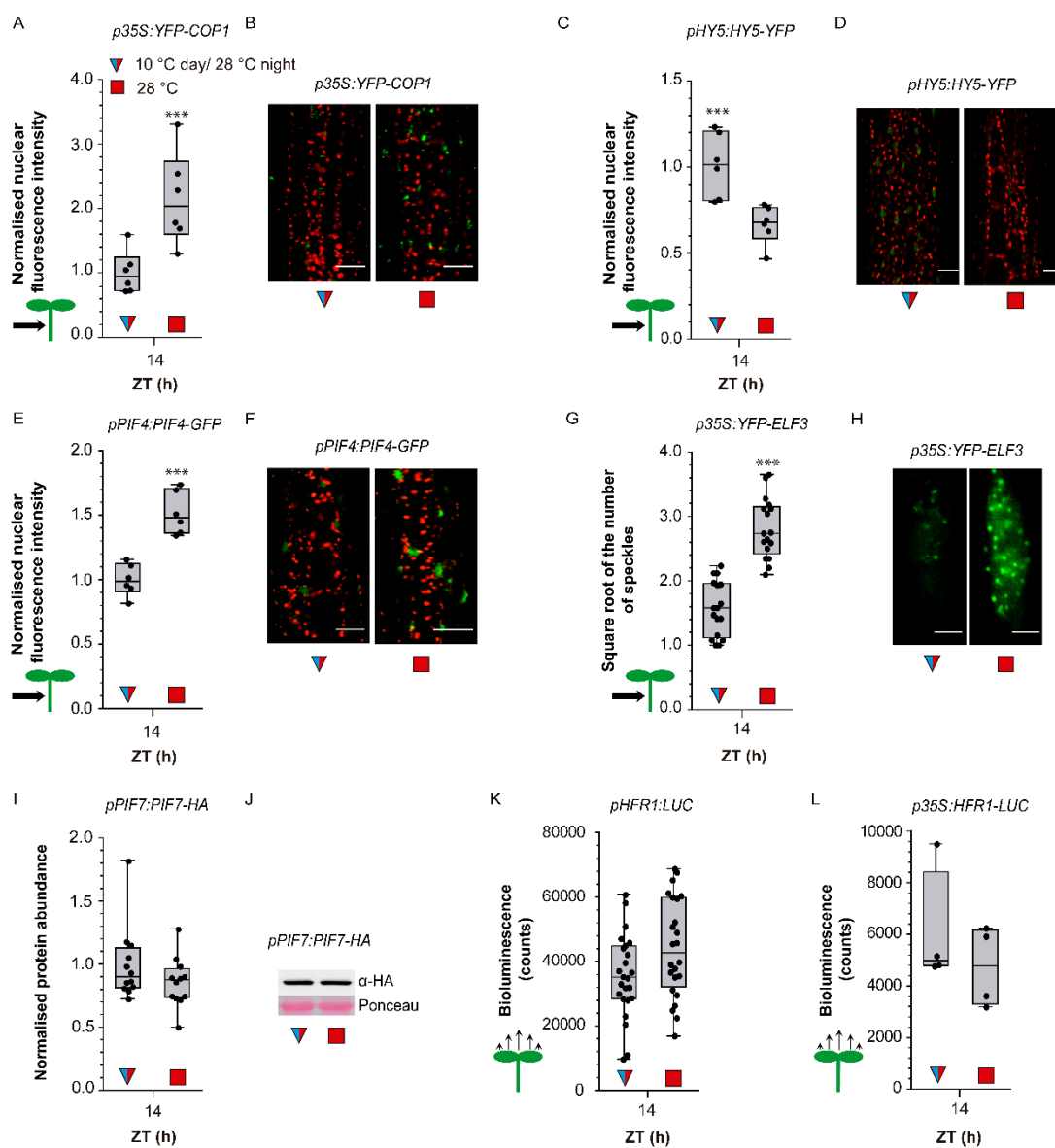


**Figure 4.** Daytime temperatures affect nighttime signalling status.

**(A-B)** Nuclear fluorescence driven in hypocotyl cells by *p35S:YFP-COP1*.

**(C-D)** Nuclear fluorescence driven in hypocotyl cells by *pHY5:HY5-YFP*.

**(E-F)** Nuclear fluorescence driven in hypocotyl cells by *pPIF4:PIF4-GFP*.

**(G-H)** Number of ELF3 nuclear speckles (square root-transformed data) in the hypocotyl cells of the line expressing the *p35S:YFP-ELF3* transgene.



**(I-J)** Abundance of PIF7 in seedlings bearing *pPIF7:PIF7-HA*.

**(K-L)** Luciferase activity driven by *pHFR1:LUC* (K) or *p35S:HFR1-LUC* (L).

The seedlings received shade and either 10°C or 28°C during the day, EOD FR and 28°C during the night. Box plots show median, interquartile range 1-3 and the maximum-minimum interval of 6 (A, C and E), 16 (G), 12 (I), 25 (K), 4 (L) biological replicates. Representative confocal (B, D, F, H) or protein blot (J) images. Scale bar = 35  $\mu\text{m}$  (B, D, F) and 2.61  $\mu\text{m}$  (H). Asterisks indicate significant differences in *t*-tests (\*,  $p < 0.05$ ; \*\*,  $p < 0.01$ ; \*\*\*,  $p < 0.001$ ).

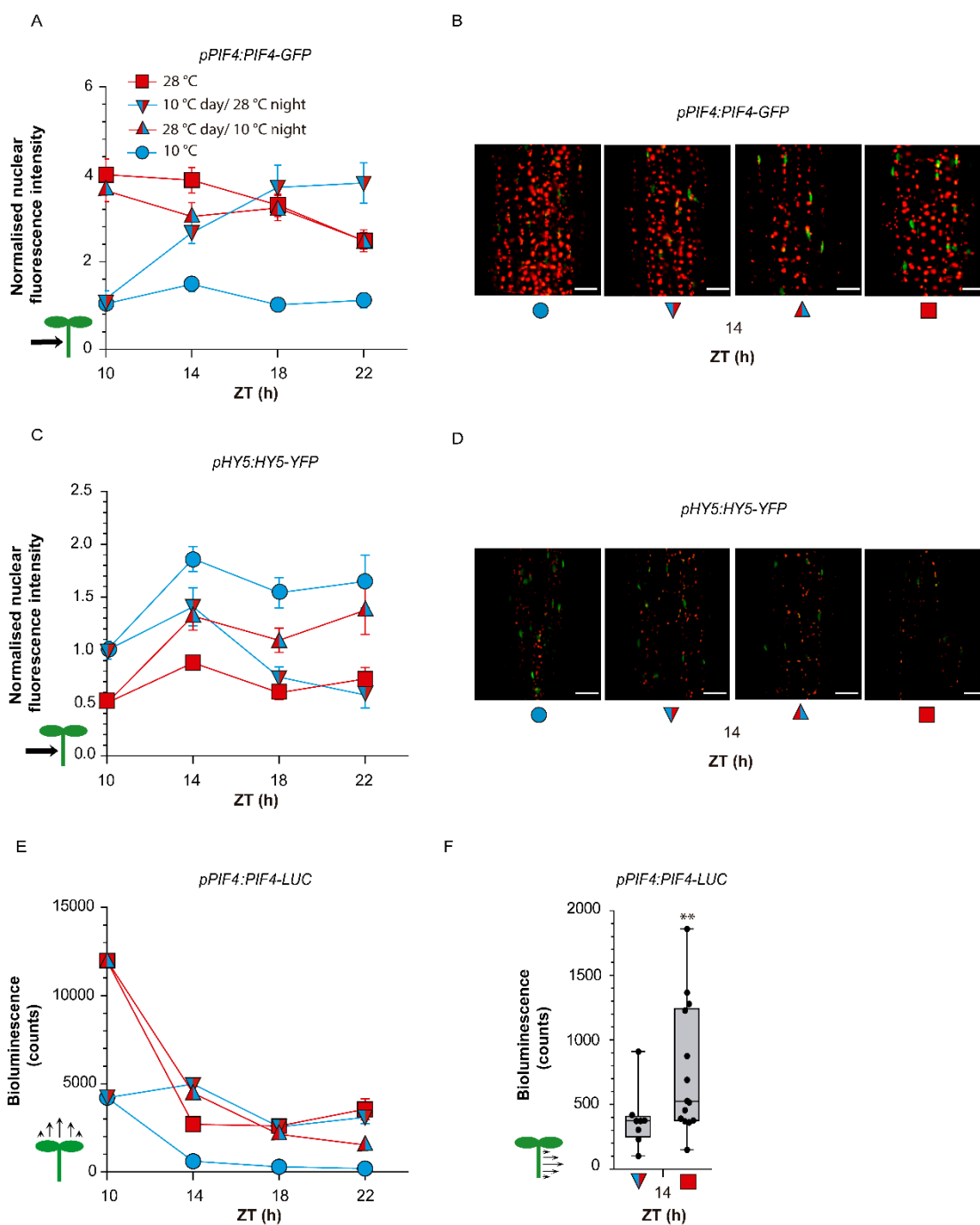


**Figure 5.** Daytime temperature affects nuclear levels of PIF4 and HY5 during the night.

(A-D) Nighttime kinetics of nuclear fluorescence intensity driven in hypocotyl cells by *pPIF4:PIF4-GFP* (A-B) or *pHY5:HY5-YFP* (C-D).

**(E)** Nighttime kinetics of luminescence driven by *pPIF4:PIF4-LUC* in entire seedlings.

**(F)** Luminescence driven by *pPIF4:PIF4-LUC* in isolated hypocotyls harvested at ZT= 14 h.

Confocal images or luminescence values were recorded during the night (starting at ZT= 10h) as affected by four combinations of daytime temperature and nighttime temperature. All seedling received shade during the day and EOD FR. (A, C, E) Data are means  $\pm$  SE of three biological replicates. (F) Box plots show median, interquartile range 1-3 and the maximum-minimum interval of 10-14 biological replicates. (B, D) Representative confocal images at ZT= 14h. Scale bar = 35  $\mu$ m. See Table S1G-I for detailed statistics of (A, C, E). In (F), the asterisks indicates significant differences in *t*-test (\*\*,  $p < 0.01$ ).

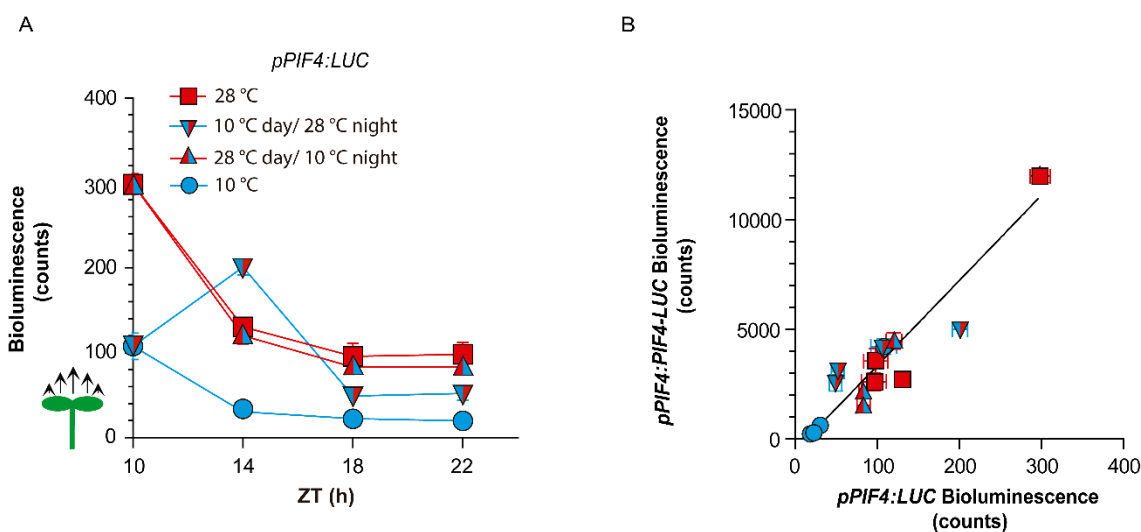


**Figure 6.** Changes in PIF4 promoter activity account for nighttime PIF4 protein dynamics.

**(A)** Nighttime kinetics of luminescence driven by *pPIF4:LUC* in entire seedlings. Luminescence was recorded during the night (starting at ZT= 10h) as affected by four combinations of daytime temperature (10 or 28°C) and nighttime temperature (10 or 28°C). All seedling received shade during the day and EOD FR. Data are means  $\pm$  SE of three plates with seedlings. See Table S1J-K for detailed statistics.

**(B)** Correlation between luminescence driven by *pPIF4:PIF4-LUC* (from 5E) and *pPIF4:LUC* (from A) in the Col-0 background. The correlation is significant at  $P < 0.0001$ .

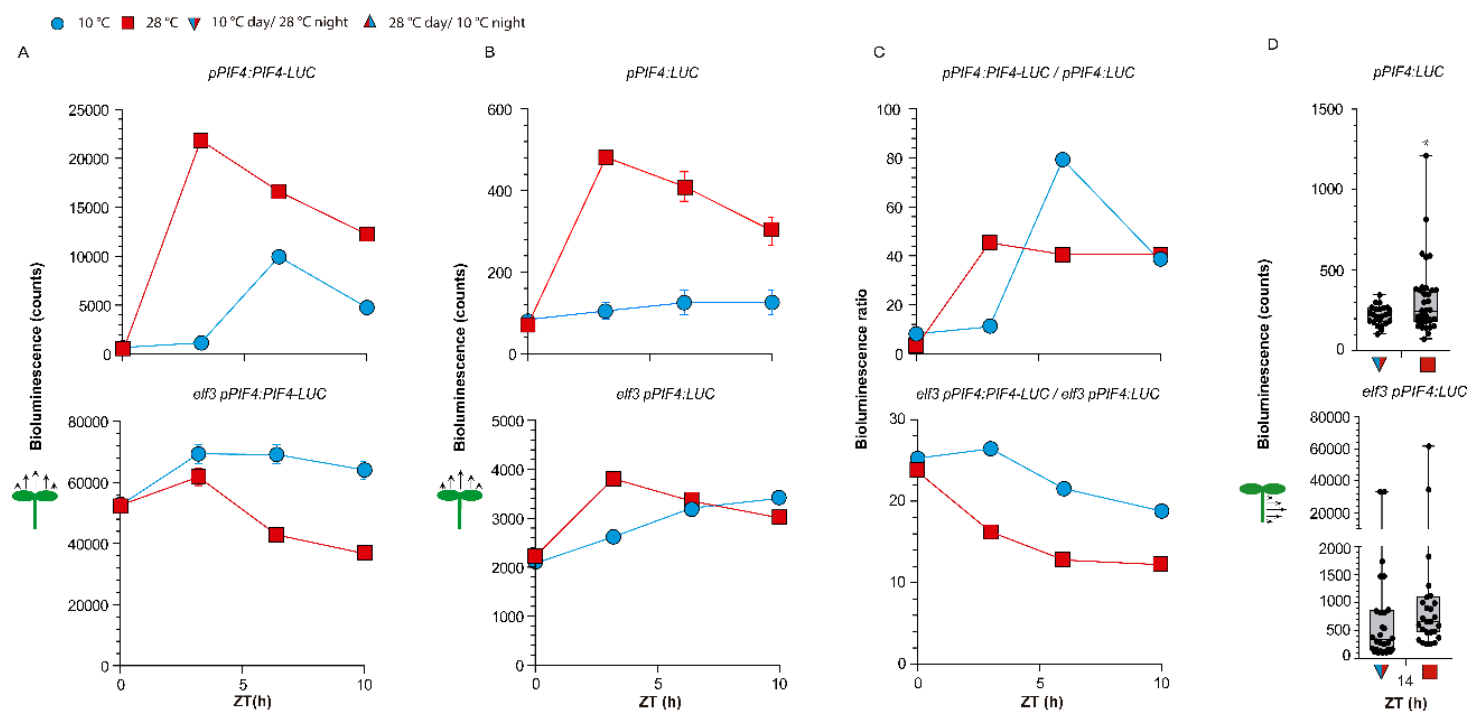


**Figure 7.** Temperature effects on end-of-day *PIF4* promoter activity and PIF4 protein abundance require ELF3.

**(A-B)** Time course of daytime luciferase activity driven by *pPIF4:PIF4-LUC* (A) or *pPIF4:LUC* (B) in the Col-0 and *elf3-8* background, as affected by 10°C or 28°C.

**(C)** Ratio between the luciferase signals driven by *pPIF4:PIF4-LUC* and *pPIF4:LUC*.

**(D)** Luminescence driven by *pPIF4:LUC* in isolated hypocotyls harvested from Col-0 and *elf3-8* seedlings at ZT= 14 h.

All seedling received shade during the day and EOD FR. (A-B) Data are means  $\pm$  SE of 3 plates with seedlings. (D) Box plots show median, interquartile range 1-3 and the maximum-minimum interval of 24-30 biological replicates, asterisk indicates significant differences in *t*-tests (\*,  $p < 0.05$ ). See Table S1L-M for detailed statistics of (A-B).

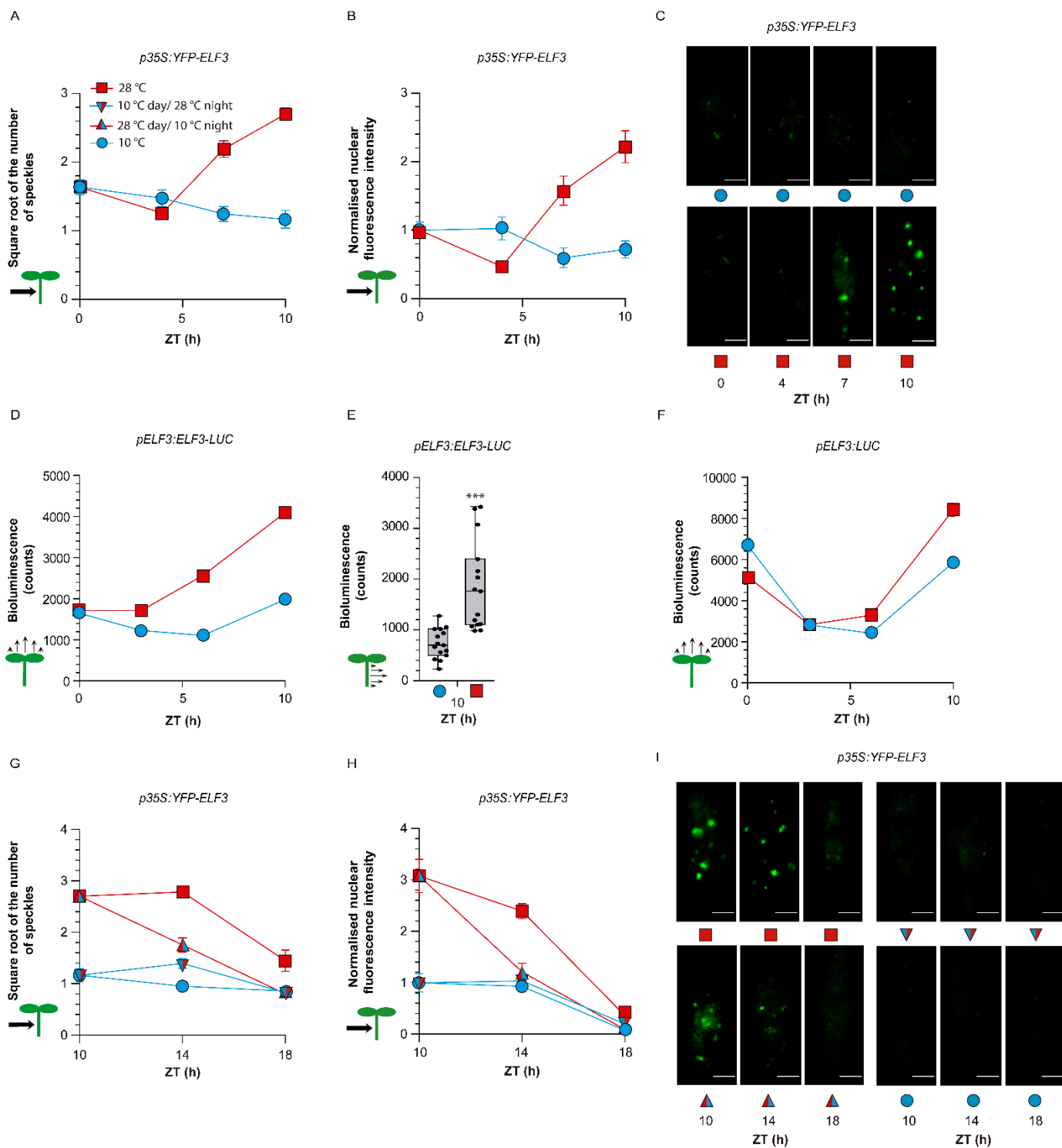


**Figure 8.** ELF3 dynamics under contrasting temperatures.

**(A-C)** Number of ELF3 nuclear speckles (A), nuclear fluorescence intensity (B) and representative confocal images (C) from hypocotyl cells of seedlings expressing *p35S:YFP-ELF3*.

**(D)** Luciferase activity driven by *pELF3:ELF3-LUC* in entire seedlings.

**(E)** Luciferase activity driven by *pELF3:ELF3-LUC* in isolated hypocotyls.

**(F)** Luciferase activity driven by *pELF3:LUC* in entire seedlings.

**(G-I)** Number of ELF3 nuclear speckles (square root-transformed data, G), nuclear fluorescence intensity (H) and representative confocal images (I) from hypocotyl cells of seedlings expressing *p35S:YFP-ELF3*.

All seedling received shade during the day and EOD FR. (A-B and G-H) Data are means  $\pm$  SE of 20 biological replicates. (C and I) Representative confocal images. Scale bar = 2.61  $\mu$ m. (D and F) Data are means  $\pm$  SE of three plates with seedlings. (E) Box plots show median, interquartile range 1-3 and the maximum-minimum interval of 15 biological replicates. See Table S1N-S for detailed statistics of (A-B, D, F-H). In E, asterisks indicate significant differences in *t*-test (\*\*\*,  $p < 0.001$ ).

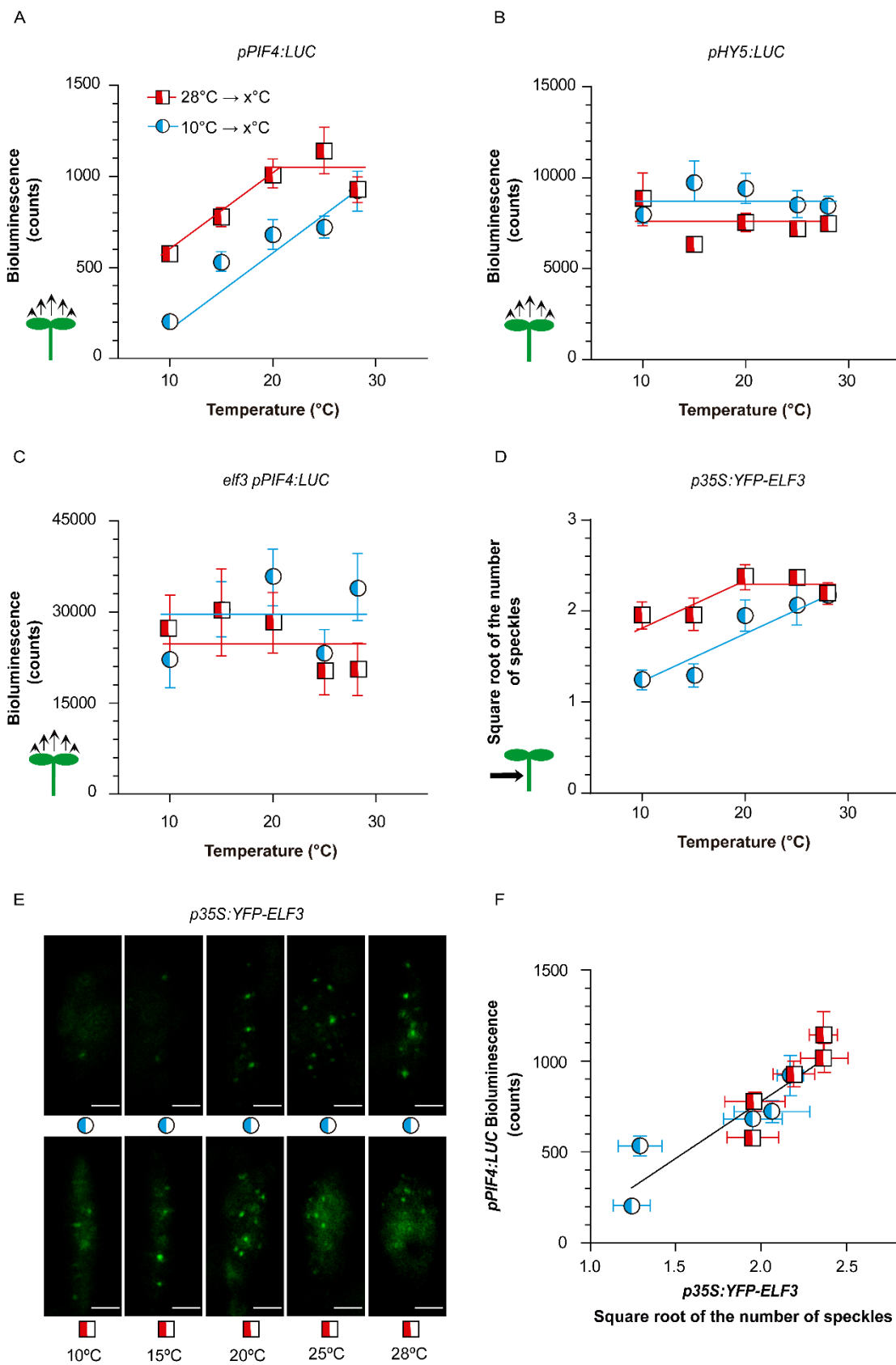




**Figure 9.** Hysteresis of ELF3 drives hysteresis in *PIF4* promoter activity.

**(A-C)** Response of the luminescence driven by *pPIF4:LUC* (A and C) or *pHY5:LUC* (B) in the Col-0 (A-B) or *elf3* (C) backgrounds to increasing or decreasing temperature.

**(D-E)** Response of the number of ELF3 nuclear speckles (square root-transformed data) from hypocotyl cells of seedlings expressing *p35S:YFP-ELF3* to increasing or decreasing temperature.

**(F)** Correlation between luminescence driven by *pPIF4:LUC* (from A) and the number of speckles driven by *p35S:YFP-ELF3* (from D).

The seedlings were exposed to white light at either 10°C or 28°C and 4 h after the beginning of the photoperiod were transferred to the temperature indicated in abscissas (including controls that remained at 10°C or 28°C). Luminescence (A-C) or confocal images (D and E) were taken 3 h later. Data are means  $\pm$  SE of 3 plates with seedlings (A-C) or 15 biological replicates (D and E). (E) Representative confocal images. Scale bar = 2.61  $\mu$ m. In F, the correlation is significant at  $P = 0.0002$ . See Table S1T-X for detailed statistics.

## Parsed Citations

**Anwer, M.U., Davis, A., Davis, S.J., and Quint, M. (2020).** Photoperiod sensing of the circadian clock is controlled by EARLY FLOWERING 3 and GIGANTEA. *Plant J.* 101: 1397–1410.

Google Scholar: [Author Only](#) [Title Only](#) [Author and Title](#)

**Bellstaedt, J., Trenner, J., Lippmann, R., Poeschl, Y., Zhang, X., Friml, J., Quint, M., and Delker, C. (2019).** A mobile auxin signal connects temperature sensing in cotyledons with growth responses in hypocotyls. *Plant Physiol.* 180: 757–766.

Google Scholar: [Author Only](#) [Title Only](#) [Author and Title](#)

**Bours, R., Kohlen, W., Bouwmeester, H.J., and van der Krol, A. (2015).** Thermoperiodic control of hypocotyl elongation depends on auxin-induced ethylene signaling that controls downstream PHYTOCHROME INTERACTING FACTOR3 activity. *Plant Physiol.* 167: 517–30.

Google Scholar: [Author Only](#) [Title Only](#) [Author and Title](#)

**Bours, R., van Zanten, M., Pierik, R., Bouwmeester, H., and van der Krol, A. (2013).** Antiphase light and temperature cycles affect PHYTOCHROME B-controlled ethylene sensitivity and biosynthesis, limiting leaf movement and growth of Arabidopsis. *Plant Physiol.* 163: 882–95.

Google Scholar: [Author Only](#) [Title Only](#) [Author and Title](#)

**Box, M.S. et al. (2015).** ELF3 controls thermoresponsive growth in Arabidopsis. *Curr. Biol.* 25: 194–199.

Google Scholar: [Author Only](#) [Title Only](#) [Author and Title](#)

**Burgie, E.S., Gannam, Z.T.K., McLoughlin, K.E., Sherman, C.D., Holehouse, A.S., Stankey, R.J., and Vierstra, R.D. (2021).** Differing biophysical properties underpin the unique signaling potentials within the plant phytochrome photoreceptor families. *Proc. Natl. Acad. Sci.* 118: e2105649118.

Google Scholar: [Author Only](#) [Title Only](#) [Author and Title](#)

**Van Buskirk, E.K., Reddy, A.K., Nagatani, A., and Chen, M. (2014).** Photobody localization of phytochrome B is tightly correlated with prolonged and light-dependent inhibition of hypocotyl elongation in the dark. *Plant Physiol.* 165: 595–607.

Google Scholar: [Author Only](#) [Title Only](#) [Author and Title](#)

**Casal, J.J. and Balasubramanian, S. (2019).** Thermomorphogenesis. *Annu. Rev. Plant Biol.* 70: 321–346.

Google Scholar: [Author Only](#) [Title Only](#) [Author and Title](#)

**Catalá, R., Medina, J., and Salinas, J. (2011).** Integration of low temperature and light signaling during cold acclimation response in Arabidopsis. *Proc. Natl. Acad. Sci. U. S. A.* 108: 16475–16480.

Google Scholar: [Author Only](#) [Title Only](#) [Author and Title](#)

**Cheng, M.-C., Kathare, P.K., Paik, I., and Huq, E. (2021).** Phytochrome Signaling Networks. *Annu. Rev. Plant Biol.* 72: 217–244.

Google Scholar: [Author Only](#) [Title Only](#) [Author and Title](#)

**Chung, B.Y.W., Balcerowicz, M., Di Antonio, M., Jaeger, K.E., Geng, F., Franaszek, K., Marriott, P., Brierley, I., Firth, A.E., and Wigge, P.A. (2020).** An RNA thermoswitch regulates daytime growth in Arabidopsis. *Nat. Plants* 6: 522–532.

Google Scholar: [Author Only](#) [Title Only](#) [Author and Title](#)

**Crawford, A.J., McLachlan, D.H., Hetherington, A.M., and Franklin, K.A. (2012).** High temperature exposure increases plant cooling capacity. *Curr. Biol.* 22: R396-7.

Google Scholar: [Author Only](#) [Title Only](#) [Author and Title](#)

**Davies, J. (2017).** Using synthetic biology to explore principles of development. *Dev.* 144: 1146–1158.

Google Scholar: [Author Only](#) [Title Only](#) [Author and Title](#)

**Delker, C. et al. (2014).** The DET1-COP1-HY5 pathway constitutes a multipurpose signaling module regulating plant photomorphogenesis and thermomorphogenesis. *Cell Rep.* 9: 1983–1989.

Google Scholar: [Author Only](#) [Title Only](#) [Author and Title](#)

**Ding, L., Wang, S., Song, Z.T., Jiang, Y., Han, J.J., Lu, S.J., Li, L., and Liu, J.X. (2018).** Two B-Box Domain Proteins, BBX18 and BBX23, Interact with ELF3 and Regulate Thermomorphogenesis in Arabidopsis. *Cell Rep.* 25: 1718-1728.e4.

Google Scholar: [Author Only](#) [Title Only](#) [Author and Title](#)

**Emenecker, R.J., Holehouse, A.S., and Strader, L.C. (2021).** Biological Phase Separation and Biomolecular Condensates in Plants. *Annu. Rev. Plant Biol.* 72: 17–46.

Google Scholar: [Author Only](#) [Title Only](#) [Author and Title](#)

**Ezer, D. et al. (2017).** The evening complex coordinates environmental and endogenous signals in Arabidopsis. *Nat. Plants* 3: 17087.

Google Scholar: [Author Only](#) [Title Only](#) [Author and Title](#)

**Fehér, B., Kozma-Bognár, L., Kevei, É., Hajdu, A., Binkert, M., Davis, S.J., Schäfer, E., Ulm, R., and Nagy, F. (2011).** Functional interaction of the circadian clock and UV RESISTANCE LOCUS 8-controlled UV-B signaling pathways in Arabidopsis thaliana. *Plant J.* 67: 37–48.

Google Scholar: [Author Only](#) [Title Only](#) [Author and Title](#)

**Fiorucci, A.-S., Galvão, V.C., Ince, Y.Ç., Boccaccini, A., Goyal, A., Allenbach Petrolati, L., Trevisan, M., and Fankhauser, C. (2020). PHYTOCHROME INTERACTING FACTOR 7 is important for early responses to elevated temperature in Arabidopsis seedlings. *New Phytol.* 226: 50–58.**

Google Scholar: [Author Only](#) [Title Only](#) [Author and Title](#)

**Foreman, J., Johansson, H., Hornitschek, P., Josse, E.-M.M., Fankhauser, C., and Halliday, K.J. (2011). Light receptor action is critical for maintaining plant biomass at warm ambient temperatures. *Plant J.* 65: 441–452.**

Google Scholar: [Author Only](#) [Title Only](#) [Author and Title](#)

**Gangappa, S.N. and Kumar, S.V. (2017). DET1 and HY5 Control PIF4-Mediated Thermosensory Elongation Growth through Distinct Mechanisms. *Cell Rep.* 18: 344–351.**

Google Scholar: [Author Only](#) [Title Only](#) [Author and Title](#)

**Gray, W.M., Östin, A., Sandberg, G., Romano, C.P., and Estelle, M. (1998). High temperature promotes auxin-mediated hypocotyl elongation in Arabidopsis. *Proc. Natl. Acad. Sci. U. S. A.* 95: 7197–7202.**

Google Scholar: [Author Only](#) [Title Only](#) [Author and Title](#)

**Herrero, E. et al. (2012). EARLY FLOWERING4 recruitment of EARLY FLOWERING3 in the nucleus sustains the Arabidopsis circadian clock. *Plant Cell* 24: 428–43.**

Google Scholar: [Author Only](#) [Title Only](#) [Author and Title](#)

**Hornitschek, P., Lorrain, S., Zoete, V., Michielin, O., and Fankhauser, C. (2009). Inhibition of the shade avoidance response by formation of non-DNA binding bHLH heterodimers. *EMBO J.* 28: 3893–3902.**

Google Scholar: [Author Only](#) [Title Only](#) [Author and Title](#)

**Huq, E. and Quail, P. (2002). PIF4, a phytochrome-interacting bHLH factor, functions as a negative regulator of phytochrome B signaling in Arabidopsis. *EMBO J.* 21: 2441–2450.**

Google Scholar: [Author Only](#) [Title Only](#) [Author and Title](#)

**Jiang, Y. and Hao, N. (2021). Memorizing environmental signals through feedback and feedforward loops. *Curr. Opin. Cell Biol.* 69: 96–102.**

Google Scholar: [Author Only](#) [Title Only](#) [Author and Title](#)

**Jung, J.-H. et al. (2016). Phytochromes function as thermosensors in Arabidopsis. *Science* (80-. ). 354: 886–889.**

Google Scholar: [Author Only](#) [Title Only](#) [Author and Title](#)

**Jung, J.H. et al. (2020). A prion-like domain in ELF3 functions as a thermosensor in Arabidopsis. *Nature* 585: 256–260.**

Google Scholar: [Author Only](#) [Title Only](#) [Author and Title](#)

**Kim, J., Lee, H., Lee, H.G., and Seo, P.J. (2021). Get closer and make hotspots: liquid–liquid phase separation in plants. *EMBO Rep.* 22: 1–15.**

Google Scholar: [Author Only](#) [Title Only](#) [Author and Title](#)

**Koini, M.A., Alvey, L., Allen, T., Tilley, C. a, Harberd, N.P., Whitlam, G.C., and Franklin, K. a (2009). High temperature-mediated adaptations in plant architecture require the bHLH transcription factor PIF4. *Curr. Biol.* 19: 408–13.**

Google Scholar: [Author Only](#) [Title Only](#) [Author and Title](#)

**Legris, M., Klose, C., Burgie, E., Costigliolo Rojas, C., Neme, M., Hiltbrunner, A, Wigge, P.A, Schäfer, E., Vierstra, R.D., and Casal, J.J. (2016). Phytochrome B integrates light and temperature signals in Arabidopsis. *Science* (80-. ). 354: 897–900.**

Google Scholar: [Author Only](#) [Title Only](#) [Author and Title](#)

**Legris, M., Nieto, C., Sellaro, R., Prat, S., and Casal, J.J. (2017). Perception and signalling of light and temperature cues in plants. *Plant J.* 90: 683–697.**

Google Scholar: [Author Only](#) [Title Only](#) [Author and Title](#)

**Murcia, G., Enderle, B., Hiltbrunner, A, and Casal, J.J. (2020). Phytochrome B and PCH1 protein dynamics store night temperature information. *Plant J.*: in press.**

Google Scholar: [Author Only](#) [Title Only](#) [Author and Title](#)

**Nieto, C., López-Salmerón, V., Davière, J.-M., and Prat, S. (2015). ELF3-PIF4 interaction regulates plant growth independently of the Evening Complex. *Curr. Biol.* 25: 187–93.**

Google Scholar: [Author Only](#) [Title Only](#) [Author and Title](#)

**Nusinow, D. a, Helfer, A, Hamilton, E.E., King, J.J., Imaizumi, T., Schultz, T.F., Farré, E.M., and Kay, S. a (2011). The ELF4-ELF3-LUX complex links the circadian clock to diurnal control of hypocotyl growth. *Nature* 475: 398–402.**

Google Scholar: [Author Only](#) [Title Only](#) [Author and Title](#)

**Park, Y.-J., Lee, H.-J., Ha, J.-H., Kim, J.Y., and Park, C.-M. (2017). COP1 conveys warm temperature information to hypocotyl thermomorphogenesis. *New Phytol.* 215: 269–280.**

Google Scholar: [Author Only](#) [Title Only](#) [Author and Title](#)

**Press, M.O., Lanctot, A, and Queitsch, C. (2016). PIF4 and ELF3 act independently in Arabidopsis thaliana thermoresponsive flowering. *PLoS One* 11: 14–16.**

Google Scholar: [Author Only](#) [Title Only](#) [Author and Title](#)

- Quint, M., Delker, C., Franklin, K.A., Wigge, P.A., Halliday, K.J., and van Zanten, M. (2016). Molecular and genetic control of plant thermomorphogenesis. *Nat. Plants* 2: 15190.  
Google Scholar: [Author Only Title Only Author and Title](#)
- Quiroz, F.G., Li, N.K., Roberts, S., Weber, P., Dzuricky, M., Weitzhandler, I., Yingling, Y.G., and Chilkoti, A. (2019). Intrinsically disordered proteins access a range of hysteretic phase separation behaviors. *Sci. Adv.* 5: 1–12.  
Google Scholar: [Author Only Title Only Author and Title](#)
- Raschke, A. et al. (2015). Natural variants of ELF3 affect thermomorphogenesis by transcriptionally modulating PIF4-dependent auxin responses. *BMC Plant Biol.* 15: 197.  
Google Scholar: [Author Only Title Only Author and Title](#)
- Rausenberger, J., Hussong, A., Kircher, S., Kirchenbauer, D., Timmer, J., Nagy, F., Schäfer, E., and Fleck, C. (2010). An integrative model for phytochrome B mediated photomorphogenesis: from protein dynamics to physiology. *PLoS One* 5: e10721.  
Google Scholar: [Author Only Title Only Author and Title](#)
- Reichert, P. and Caudron, F. (2021). Mnemons and the memorization of past signaling events. *Curr. Opin. Cell Biol.* 69: 127–135.  
Google Scholar: [Author Only Title Only Author and Title](#)
- Romero-Montepaone, S., Sellaro, R., Hernando, C.E., Costigliolo-Rojas, C., Bianchimano, L., Ploschuk, E.L., Yanovsky, M.J., and Casal, J.J. (2021). Functional convergence of growth responses to shade and warmth in *Arabidopsis*. *New Phytol.*: doi.org/10.1111/nph.17430.  
Google Scholar: [Author Only Title Only Author and Title](#)
- Ronald, J., Wilkinson, A.J., and Davis, S.J. (2021). EARLY FLOWERING3 sub-nuclear localization responds to changes in ambient temperature. *Plant Physiol.*: 1–4.  
Google Scholar: [Author Only Title Only Author and Title](#)
- Sandi Paulišić, Qin, W., Harshul Arora Verasztó, C.T., Nogue, B., Alary, F., Tsiantis, M., Hothorn, M., and Martínez-García, J.F. (2021). Adjustment of the PIF7-HFR1 transcriptional module activity controls plant shade adaptation. *EMBO J.* 40: e104273.  
Google Scholar: [Author Only Title Only Author and Title](#)
- Sellaro, R., Smith, R.W., Legris, M., Fleck, C., and Casal, J.J. (2019). Phytochrome B dynamics departs from photoequilibrium in the field. *Plant. Cell Environ.* 42: 606–617.  
Google Scholar: [Author Only Title Only Author and Title](#)
- Silva, C.S., Nayak, A., Lai, X., Hutin, S., Hugouvieux, V., Jung, J.-H., López-Vidriero, I., Franco-Zorrilla, J.M., Panigrahi, K.C.S., Nanao, M.H., Wigge, P.A., and Zubieta, C. (2020). Molecular mechanisms of Evening Complex activity in *Arabidopsis*. *Proc. Natl. Acad. Sci. U. S. A.* 117: 6901–6909.  
Google Scholar: [Author Only Title Only Author and Title](#)
- Stavang, J.A., Gallego-Bartolomé, J., Gómez, M.D., Yoshida, S., Asami, T., Olsen, J.E., García-Martínez, J.L., Alabadí, D., and Blázquez, M.A. (2009). Hormonal regulation of temperature-induced growth in *Arabidopsis*. *Plant J.* 60: 589–601.  
Google Scholar: [Author Only Title Only Author and Title](#)
- Sun, J., Qi, L., Li, Y., Chu, J., and Li, C. (2012). PIF4-mediated activation of YUCCA8 expression integrates temperature into the auxin pathway in regulating *Arabidopsis* hypocotyl growth. *PLoS Genet.* 8: e1002594.  
Google Scholar: [Author Only Title Only Author and Title](#)
- Thines, B. and Harmon, F.G. (2010). Ambient temperature response establishes ELF3 as a required component of the core *Arabidopsis* circadian clock. *Proc. Natl. Acad. Sci. U. S. A.* 107: 3257–3262.  
Google Scholar: [Author Only Title Only Author and Title](#)
- Toledo-Ortiz, G., Johansson, H., Lee, K.P., Bou-Torrent, J., Stewart, K., Steel, G., Rodríguez-Concepción, M., and Halliday, K.J. (2014). The HY5-PIF regulatory module coordinates light and temperature control of photosynthetic gene transcription. *PLoS Genet.* 10: e1004416.  
Google Scholar: [Author Only Title Only Author and Title](#)
- Zhang, L.L., Li, W., Tian, Y.Y., Davis, S.J., and Liu, J.X. (2021). The E3 ligase XBAT35 mediates thermoresponsive hypocotyl growth by targeting ELF3 for degradation in *Arabidopsis*. *J. Integr. Plant Biol.* 63: 1097–1103.  
Google Scholar: [Author Only Title Only Author and Title](#)
- Zhu, J.-Y., Oh, E., Wang, T., and Wang, Z.-Y. (2016). TOC1–PIF4 interaction mediates the circadian gating of thermoresponsive growth in *Arabidopsis*. *Nat. Commun.* 7: 13692.  
Google Scholar: [Author Only Title Only Author and Title](#)